

İSTANBUL UNIVERSITY-CERRAHPAŞA
INSTITUTE OF GRADUATE STUDIES



M.Sc. THESIS

DESIGN OPTIMIZATION OF A HYBRID VIBRATION CONTROL SYSTEM FOR BUILDINGS STRUCTURES

Basel SALAAS

SUPERVISOR
Prof. Dr. Gebrail BEKDAŞ

CO-SUPERVISOR
Prof. Dr. Yasser MANSOUR

Drpartment of Civil Engineering

Civil Engineering Program

January, 2023

THESIS ACCEPTANCE AND APPROVAL

This thesis entitled as *" **DESIGN OPTIMIZATION of a HYBRID VIBRATION CONTROL SYSTEM for BUILDINGS STRUCTURES** "*, prepared by **Basel SALAAS** under the supervision of **Prof. Dr. Gebrail BEKDAŞ** , was accepted as a **M.Sc. Thesis** after being **consensus** approved by our jury as a result of the exam held on **05/01/2023 at 10:00 AM**.

Examining Committee Members

		Signature	Decision
SUPERVISOR	Prof. Dr. Gebrail BEKDAŞ Istanbul University- Cerrahpaşa Civil Engineering Department		☐ Accept ☐ Reject
MEMBER	Assoc. Prof. Dr. Sinan Melih NIGDELI Istanbul University- Cerrahpaşa Civil Engineering Department		☐ Accept ☐ Reject
MEMBER	Assoc. Prof. Dr. Serdar ÇARBAŞ Karamanoğlu Mehmet Bey University Civil Engineering Department		☐ Accept ☐ Reject

DECLARATION

I hereby declare that this thesis is my own work and I have not had engaged in any unethical behavior at any of the stages from planning to the writing of the thesis. I have obtained all the information in this thesis within the limits of the academic and scientific ethical rules, I have cited all the information and comments being obtained in this thesis study, and I have included these references in the list of references. During the analysis and writing stages of this thesis, I have abided by the patent and copyright rights; therefore, I myself take all kinds of legal responsibility.

Basel SALAAS

(Signature)

To my mother, father, family and thesis advisors …

FUNDING

DESIGN OPTIMIZATION of a HYBRID VIBRATION CONTROL SYSTEM for BUILDINGS STRUCTURES

This thesis was supported by the Research and Initiatives Center, Prince Sultan University, Saudi Arabia in 2022.

ACKNOWLEDGEMENT

I would like to extend my sincere thanks and appreciation to my supervisor Prof. Dr. Gebrail BEKDAŞ and Assoc. Prof. Dr. Sinan Melih NIGDELI for their guidance throughout my thesis period. Their efforts and support are extremely appreciated. Special thanks to my co-supervisor Prof. Dr. Yasser MANSOUR for his full support and for believing in me. Many thanks to my nephews Nada, Qusay, Leen and Hala for their encouragement and help. I am also grateful to my best friend Tarık SEYIT who did not hesitate to help since ever I knew him. No words can explain my gratitude to all my family, especially my mother Khadijah and my father Kamal who raised me, taught me and gave me opportunities that they did not even dream of themselves. I would like also to thank my sister Hanaa for taking care of me in the tough times during my academic journey.

January, 2023 Basel SALAAS

CONTENTS

Page

THESIS ACCEPTANCE AND APPROVAL ..... **ii**
DECLARATION ..... **iii**
FUNDING ..... **v**
ACKNOWLEDGEMENT ..... **vi**
CONTENTS ..... **vii**
LIST OF FIGURES ..... **ix**
LIST OF TABLES ..... **xii**
LIST OF SYMBOLS AND ABBREVIATIONS ..... **xv**
GENİŞLETİLMİŞ ÖZET ..... **xvii**
ABSTRACT ..... **xviii**
1. INTRODUCTION **1**
1.1. OBJECTIVE AND IMPORTANCE OF STUDY 3
1.2. SCOPE AND STRUCTURE OF STUDY 4
2. CONCEPTUAL FRAMEWORK **5**
2.1. LITERATURE REVIEW 5
2.2. SEISMIC ISOLATION 9
2.2.1. Principle of Seismic Isolation 9
2.2.2. Types of Isolation Systems 10
2.3. TUNED LIQUID COLUMN DAMPER 10
2.3.1. Geometry of TLCD 11
2.3.2. The Efficacy of TLCD 11
2.3.3. Advantages of TLCD 12
2.3.4. Modeling of TLCD 12
2.3.4.1. TLCD's Equation of Motion for Reducing Single-Direction Vibration 12
2.3.4.2. TLCD's Equation of Motion for Reducing Coupled Translation and Rotation Vibrations 13

2.4. APPROXIMATE SUBSTRUCTURE SYNTHESIS 14
2.4.1. TLCD/TMD in Symmetric Structure.....15
2.4.2. TLCD/TMD in Asymmetric Structure 16
3. METHOD.....20
3.1. MODAL TUNING OF TLCD 20
3.1.1. Similarity between TLCD and TMD when Used in Symmetric Structure 20
3.1.2. Similarity between TLCD and TMD when Used in Asymmetric Structure 22
3.1.3. The Metaheuristic Algorithm-Based Optimization 23
4. RESULTS.....26
5. DISCUSSION.....39
6. CONCLUSION AND RECOMMENDATIONS 42
REFERENCES 46
FIRST PAGE OF THE PLAGIARISM REPORT.....52
ETHICS COMMITTEE PERMISSION.....53
INSTITUTIONAL PERMISSIONS 54
CURRICULUM VITAE 55

LIST OF FIGURES

Page

Figure 1: Tuned Liquid Column Damper Geometry.....11

Figure 2: Base-isolated MDOF shear-type frame Structures: (a) without TLCD (b) with TLCD.....29

Figure 3: Peak Responses for hybrid-controlled structure, base-isolated structure and simple uncontrolled structure subjected to earthquake no.37 record.....32

Figure 4: Peak responses for a hybrid-controlled structure, base-isolated structure and simple uncontrolled structure subjected to earthquake no.21 record.....33

Figure 5: Two ground acceleration records of the FEMA P-695-FF set: a) Earthquake no.21; b) Earthquake no.37 34

Figure 6: Response time histories of roof level for the earthquake-prone simple uncontrolled structure, base-isolated structure and hybrid controlled structure (eqrthquake no. 37 record).....35

Figure 7: Response time histories of base level for the earthquake-prone simple uncontrolled structure, base-isolated structure, and hybrid controlled structure (eartquuake no. 37 record).....36

Figure 8: Response time histories of roof level for the earthquake-prone simple uncontrolled structure, base-isolated structure, and hybrid controlled structure (earthquake no. 21 record).....37

Figure 9: Response time histories of base level for the earthquake-prone simple uncontrolled structure, base-isolated structure, and hybrid controlled structure (earthquake no. 21 record).....38

LIST OF TABLES

Page

Table 1: JAYA Optimization Components 24

Table 2: Examples for The Structurl Responses of Base and Roof Levels 27

Table 3: Properties of Optimized Base-Isolated Subsystem 28

Table 4: Properties Of Optimized TLCD System 30

Table 5: The Maximum Structural Responses of Base and Roof Levels Under 44 Earthquaks Effects for The Hybrid Controlled Structure 31

LIST OF SYMBOLS AND ABBREVIATIONS

Symbols	Description
B	: Liquid columns' horizontal length
H	: Liquid columns' inclined length
AB	: Horizontal liquid columns' cross-sectional area
AH	: Inclined liquid columns' cross-sectional area
u1, u2, u(t)	: Displacement of liquid column
$\ddot{w}_g$	: Ground acceleration
ρ	: Liquid density
p_1, p_2	: Air pressure at the free surfaces
p_0	: Ambient pressure
Δp	: Change in pressure
Δp_L	: Pressure loss along the streamline
Re	: Reynolds number
R	: Characteristic cross sectional dimension
ν	: Kinematic viscosity
$\ddot{w}$	: Floor's relative horizontal displacement)
k	: The factor of excitation influence
L_{eff}	: Liquid column's effective length
$\overrightarrow{L_J}, \overrightarrow{L^*_J}$	: Modified participation factor
ω_A	: TLCD's undamped linear natural circular frequency
ω_{sj}	: Main building's circular natural frequency
ω^*_{sj}	: Equivalent structure's circular natural frequency
ω^*_{Aj}	: Equivalent TMD's circular natural frequency
g	: Gravity's constant
F_x	: Reaction loads on the floor
F_{Ay}, F_{AZ}, M_A	: Control forces in Y, Z and θ directions

$\vec{\mathbf{F}}(\boldsymbol{t})$: wind forces

Mx : Linearized moment

$\boldsymbol{m_f}$: Total fluid mass

γ : Angle of trace of TLCD in y-direction

A : Reference point

$\widetilde{\boldsymbol{M}}$: Diagonal mass matrix

$\widetilde{\boldsymbol{C}}$: Main system's light damping matrix

$\widetilde{\boldsymbol{K}}$: Main system's stiffness matrix

$\overrightarrow{\mathbf{w}}$: Floor displacement

$\mathbf{v}_{\boldsymbol{Aij}}$: Reference point A_i modal displacement in y-directions

$\mathbf{w}_{\boldsymbol{Aij}}$: Reference point A_i modal displacement in z-directions

$\boldsymbol{m_j}$: Modal mass

$\overrightarrow{\boldsymbol{\phi_\iota}}^{\boldsymbol{T}}$: Transposed ortho-normalized modal vector

$\boldsymbol{\mu_j}$: Ratio of mass

$\boldsymbol{\xi_{sj}}$: Modal damping

$\boldsymbol{\xi_{Ajopt}}$: Optimal damping coefficient of TLCD

$\boldsymbol{\xi^*_{Ajopt}}$: Optimal damping coefficient of equivalent TMD

$\boldsymbol{\mu^*_j}$: Alternative mass ratio

$\boldsymbol{v_i}$, $\boldsymbol{w_i}$, $\boldsymbol{u_{Ti}}$: Isolated modal displacements

$\boldsymbol{m_{Sn}}$, $\boldsymbol{m^*_{Sn}}$: Mass of the floor number n

$\boldsymbol{m_j}$, $\boldsymbol{m^*_j}$: Modal mass

$\boldsymbol{\delta^*_{jopt}}$: TMD optimal frequency ratio

$\boldsymbol{\delta_{jopt}}$: TLCD optimal frequency ratio

i : Number of design variables

j : Solution vectors

Xi,j : Design value's variable

Xi(low) : Design value's lower limit

Xi(up) : Design value's upper limit

CL : Initial solution matrix

Xnew : New solution

Xsel : Selected existing solution

Xlow : Design value's lower limit

Xup : Design value's upper limit

Xbest : Best solution

Xold : Existing (old) solution

Xmean : Mean value of existing solutions

Xa, Xb : Two random solutions from the existing solutions

f (Xa), f (Xb) : Existing solution's objective function

Abbreviations **Description**

TLCD : Tuned Liquid Column Damper

TLD : Tuned liquid damper

TMD : Tuned mass damper

SDOF : Single degree of freedom

USC : University of South California

2-DOF : Two degrees of freedom

Eq : Equation

pn : Population number

rand : Random numbers

GENİŞLETİLMİŞ ÖZET

YÜKSEK LİSANS TEZİ

BİNA YAPILARI İÇİN BİR HİBRİT TİTREŞİM KONTROL SİSTEMİNİN TASARIM OPTİMİZASYONU

Basel SALAAS

İstanbul Üniversitesi-Cerrahpaşa

Lisansüstü Eğitim Enstitüsü

İnşaat Mühendisliği Anabilim Dalı

İnşaat Mühendisliği Programı

Danışman : Prof. Dr. Gebrail BEKDAŞ

II. Danışman : Prof. Dr. Yasser MANSOUR

Bu tezde, yüksek bina yapılarının sismik uyarımlar altındaki kontrolü, taban izolasyon (BI) alt sistemi ve pasif ayarlı sıvı kolon sönümleyici (TLCD) sisteminden oluşan pasif hibrit kontrol sistemi kullanılarak incelenmiştir. Her iki sistem de diğer sistemin deprem etkisindeki bir yapıda kullanılması düşünülerek özel olarak optimize edilmiştir. Yapının dinamik analizi ve metasezgisel optimizasyon yöntemlerine dayalı olarak bir optimizasyon yöntemi geliştirilmiş ve bir bilgisayar kodu yazılmıştır. TLCD ve BI tasarımı için optimal bir kontrol algoritması uygulandı. Algoritma, tabandan izole edilmiş yapılarda olduğu gibi, çok düşük bir temel doğal frekansa sahip baskın bir birinci mod ile karakterize edilen sistemler için özellikle uygundur. Çalışma kapsamında optimizasyon sürecinde birçok deprem kaydı kullanılarak genel bir çözüm bulunmuştur. Ayrıca bu çalışmada yüksek performansı ile bilinen bu projenin amacını gerçekleştirmek için en uygun ve başarılı metasezgisel algoritmalardan biri kullanılmıştır. Ek olarak, optimize edilmiş hibrit kontrol sisteminin binaların sismik davranışını kontrol etmedeki etkinliğini araştırmak için bir çok katlı bina yapısı üzerinde sayısal simülasyonlar yapılmıştır. Tabandan izole edilmiş TLCD kontrollü yapının

performansı, TLCD taban katına yerleştirildiğinde, taban uyarımları olarak kaydedilmiş 44 yer hareketi seti kullanılarak incelenmiştir. Bu çalışmadan elde edilen sonuçlara göre, pasif TLCD sisteminin taban izolasyon alt sisteminin güvenliğini ve bütünlüğünü koruma ve sürdürmede oldukça etkili olduğu görülmektedir. Ayrıca, önerilen pasif hibrit kontrol sistemi, yapının yapısal tepkilerini etkili bir şekilde azaltabilmektedir.

Ocak 2023 , 72 sayfa.

Anahtar kelimeler: Taban izolasyonlu yapı, Ayarlı sıvı kolon damperi, optimum tasarım, Hibrit kontrol sistemi, Metasezgisel algoritmalar.

ABSTRACT

M.Sc. THESIS

DESIGN OPTIMIZATION OF A HYBRID VIBRATION CONTROL SYSTEM FOR BUILDINGS STRUCTURES

Basel SALAAS

Istanbul University-Cerrahpaşa

Institute of Graduate Studies

Department of Civil Engineering

Civil Engineering Programme

Supervisor : Prof. Dr. Gebrail BEKDAŞ

Co-Supervisor: Prof. Dr. Yasser MANSOUR

In this thesis, control of high-rise building structures under seismic excitations was investigated using a passive hybrid control system consisting of a passive tuned liquid column damper (TLCD) system and base-isolation (BI) subsystem. Both of the systems were specifically optimized considering using the other system in a structure under earthquake effects. Based on dynamic analysis of the structure and metaheuristic optimization methods, an optimization method was developed and a computer code was written. An optimal control algorithm was applied for designing TLCD and BI. This technique is especially suitable for systems with a dominant initial mode with a relatively low fundamental natural frequency as in our instance of base-isolated structures. Within the scope of the study, a general solution was found by using many earthquake records during the optimization process. Besides, one of the most suitable and successful metaheuristic algorithms to fulfill the aim of this project that is known for its high performance was used in this study. In addition, numerical simulations were performed on a benchmark high-rise building structure to investigate the effectiveness of the optimized hybrid control system in controlling the seismic response of the buildings. A set

of 44 recorded ground motions as base excitations was utilized to place the TLCD in the base floor to examine the performance of the base-isolated TLCD-controlled structure. Based on the results obtained from this study, the passive TLCD system appears to be quite effective in protecting and maintaining the safety and integrity belonging to the base-isolation subsystem. Additionally, the proposed passive hybrid control system is able to effectively reduce the structural responses of the structure.

January 2023, 72 pages.

Keywords: Base-isolated Building, optimum design, TLCD, hybrid control, Metaheuristic algorithms.

1. INTRODUCTION

Earthquakes are one of nature's most dangerous hazards that occur suddenly and are unpredictable. Some earthquakes are huge and destructive, leading to catastrophes. There are approximately 11,000 deaths reported every year due to earthquakes. The massive damaging potential of the earthquake can also cause major damage to structures and the contents of the structures. Apart from the loss of lives, there is also an impact on the economy of countries due to damage to properties. [37].

For instance, on May 12, 2008, China experienced the Wenchuan earthquake on the eastern edge of Tibetan Plateau with a magnitude of 7.9 which resulted in more than 17,000 deaths, 374,643 injuries, and the destruction of many buildings [38]. On January 12, 2010, Haiti experienced the greatest earthquake ever recorded in the country with a magnitude of 7. It cantered 15 miles southwest of Port-au- Prince. According to experts, the overall damage costs were approximately $8 to $14 billion. 3 million people (approximately one-third of the population) were affected. According to government reports, 230,000 people died and 300,600 were injured. Almost all buildings in the country were damaged or collapsed [39].

Engineers are working hard to come up with solutions to prevent or keep the impact of earthquakes to a minimum. The main challenge for structural engineers is to reduce the impact of earthquakes on buildings. One of the effective strategies for protecting structures from earthquake effects and for obtaining the desired performance is to reduce the seismic demand on the system [40].

Conventionally, the seismic impact design approach was based on increasing the strength or ductility of the building. This leads to an increase in the stiffness of the structure resulting in higher floor accelerations, which causes damage to the building's contents. Previous earthquakes have shown that structures collapse or become dysfunctional when the ductility capacity of the structure is consumed. Even in cases where the building has been designed with more strength and ductility, the vibration-sensitive equipment in the structure may lose function due to high accelerations. In order to keep such equipment functional after an earthquake, engineers have adopted an alternative approach called seismic isolation [3].

The aim of seismic isolation is to reduce seismic demand instead of increasing the capacity of the structure. Introducing a flexible interface between the foundation and the base of the structure in seismically base-isolated systems decouples the superstructure from the earthquake ground motion. Earthquakes generally contain low-period or high-frequency waves. To protect the structure from damage, the isolation system increases the dominant period of the structure in order to decouple it from ground dominant shaking period. During an earthquake, an isolation system preserves structural integrity by making large displacements and by spending earthquake energy through damping, resulting in reduced floor accelerations and relative floor displacements in the superstructure. [42].

Because most of the displacement is on the base-isolation system, the structure acts like a rigid body. This leads to a great reduction in structure's displacements and accelerations, but there are significant, occasionally unwanted displacements in the base-isolation subsystem. Increasing the damping in the isolation system reduces isolator displacement and structural base shear; however, it increases floor acceleration and inter-story drift, which has a negative effect on the structure [4].

Several research efforts resorted to many different strategies to lower the base isolation subsystem's displacement range. Previous researches concluded that the base-isolated structures become more efficient when coupled with passive, active, or semi-active devices. In [5], researchers aimed to reduce the absolute base displacement by combining a class of passive nonlinear base isolators with an active control system. One step forward, other researchers proposed a passive hybrid control that comprised of a base isolator coupled with a tuned mass damper (TMD) [6]. For the first time, Hochrainer and Ziegler [7] used TLCD, another type of passive control system to control a five-story base-isolated building.

The typical model for TLCD is an SDOF system that is rigidly attached to a vibrating structure [9,10,11]. Like with a TMD, its effectiveness is dependent on the right tuning of the natural frequency and damping ratio. But contrary to the typical TMD, the TLCD response is nonlinear, making it impossible to determine the ideal damping parameters a priori without first knowing the value of the force. (see [9] and references therein).

Metaheuristics have been successfully applied to TMD as a numerical optimization method including the members of this study [14-16]; however, an exact optimization using metaheuristics has not been proposed for the optimization of TLCD positioned on base-isolated structures. The challenge is in the need to consider the properties of both base-isolators and TLCD as design variables.

1.1. OBJECTIVE AND IMPORTANCE OF STUDY

Optimization of the design of hybrid vibration control systems has attracted researchers in the last two decades. The objective of this study is to develop a method to optimize the design of vibrations control systems to ensure the safety of people, buildings and infrastructure during seismic excitations, and to prevent huge losses in the economic resources and capabilities of countries.

These control systems operate in order to dissipate the vibrations by decreasing the response of structures and bridges exposed to ground excitations and winds. Aside from safety insurance, it also raises the standard of living for people who live or work in high-rise towers by not being exposed to the feeling of the vibrations caused by wind actions.

This study aims to:

- Generate a methodology to design hybrid systems via existing metaheuristic methods.
- Improve and modify the metaheuristics in accordance with the study requirements.
- Investigate multi-cases of design constants to provide practical solutions to engineers.

1.2. SCOPE AND STRUCTURE OF STUDY

Within the scope of this thesis, dynamic analysis of a benchmark base-isolated TLCD-controlled structure was done by generating motion equations of the structure and the hybrid systems. These equations were then modeled utilizing MATLAB with Simulink. Then, an optimization code was generated for optimizing the BI subsystem and TLCD system specifically for base-isolated structures. JAYA metaheuristic algorithm was used in the optimization process. The effectiveness of the optimized hybrid control system was investigated by performing numerical simulations and comparing the results with the simple base-isolated structure without TLCD. Finally, the performance of the base-isolated TLCD-controlled structure was evaluated by applying different recorded ground motions as base excitations.

2. CONCEPTUAL FRAMEWORK

2.1. LITERATURE REVIEW

In the past two decades, vibration control has become a very attractive research field. There are three categories of control systems: passive control systems, active control systems, and semi-active control systems [1, 2].

Seismic base-isolation is one of the most popular and efficient passive control technologies for shielding rigid structures from earthquake excitation. Seismic isolation was first proposed in 1909 as a solution to protect structures and their contents located in earthquake-prone areas from the impact of earthquakes. It has been developed since then into an important industry [43].

In 1969, the Swiss engineer in Skopje former Yugoslavia designed the first rubber-isolated reinforced concrete building. Reinforced rubber bearing was not common at that time. Instead, nonreinforced rubber was used which was not only exhibiting the same vertical and horizontal rigidity but also had the characteristic of bouncing under force [44].

In the 1970s, practical base isolation systems were developed initially in New Zealand and then in California and Japan [3]. In Japan, one of the earthquake-prone countries, the application of seismic isolation didn’t start until the 1980s. The first seismically isolated building was completed in 1983. Ever since two isolated buildings exhibited excellent behavior during the Kobe earthquake of 1995, the application of seismic isolation has developed. Similar behavior for all isolated buildings was observed during the subsequent earthquakes in Japan [45].

During the 1994 Northridge earthquake, the seismically isolated University of South California (USC) Hospital performed very well. According to the sensor records obtained in the aftermath of the earthquake, it was observed that the isolation system was able to reduce the accelerations by half and filter high-frequency waves. While the hospital was left undamaged after the earthquake, another hospital on the USC Medical Campus faced severe structural damage that led to the evacuation of the hospital occupants and subsequently was

destroyed. Also, a nearby fixed-based steel structure building that served as a pharmacy was damaged [46].

In Turkey, seismic isolation was first used in Adana-Tarsus-Gaziantep Highway Project at the Ataturk viaduct. It was later used in Bolu mountain viaducts and at Atatürk Airport International Terminal where isolators were placed at the column connections with the roof of the Terminal Building. Antalya and Sabiha Gökçen Airports are the other examples where the technology was applied in Turkey. In addition to airports and viaducts, seismic isolation technic was used in strengthening Trabya hotel, Kocaeli University Medical Faculty Hospital, and Erzurum State Hospital. Seismic isolation system has been also used in the liquid natural gas depots in Ankara Metropolitan [47].

Seismic isolation became more popular in Turkey following the 2013 Technical Memorandum of the Ministry of Health that obliged seismic isolated design for hospitals with a capacity of 100 or more beds, and are located in the first and second seismic zone. Numerous hospital buildings have been recently designed and constructed with seismic isolation [48]. According to the Memorandum, no technical criteria are specified for projects or sites when deciding on the seismic isolation application to the intended hospital buildings. By 2018, the Turkish Earthquake Code started to cover the design considerations of seismically isolated buildings. [49].

Technological advancement and development of materials such as multi-layered elastomeric bearings have seen the base isolation technic gain widespread practical use. The elastomeric bearing consists of layers of rubber and thin steel plates which makes them rigid vertically and flexible horizontally, allowing large displacement during earthquakes. [50]. The most commonly used rubber isolators are natural (synthetic) rubber isolator, lead core rubber isolator and the high-damping rubber isolator [51]. In the late 1970s, rubber isolators with lead core were used in New Zealand. Subsequently, high damping rubber isolators emerged and different compositions were used to increase the shear stress 100% and the damping rate to the range of 10% to 20%. These high damping materials were first produced by the Malaysian Rubber Producers' Research Association and their first application was made for the Foothill Communities and Justice Center in California in 1985. The damping ratio of the low-damping rubber bearings is around 5% and it exhibits linear behaviour. The damping ratio of the high damping rubber bearings has been increased by approximately 10% and they

display nonlinear behaviour that can be modelled in binary linear. Unlike low and high damped rubber bearings, lead core is placed in the middle of the support of lead core bearings to achieve high damping between 10% and 20% [52].

In fact, a base-isolation subsystem virtually isolates the building from the ground. Between the structure and its foundation, a layer with high vertical and low horizontal stiffness is introduced to create decoupling. By doing so, the structural system's fundamental natural frequency is pushed out of the frequency spectrum that dominates during the earthquake [19].

One drawback is that a base-isolation subsystem would be required to withstand excessively huge displacements, which can be a limiting design constraint. One typical approach to get around this restriction is to add more damping to the isolation, but this can increase inter-story drift and acceleration of the building[4].

Some researchers began to examine the use of passive control mechanisms, such as the tuned mass damper (TMD), to enhance base-isolation systems' efficiency. In [20] and [6], it was examined how the base-isolated structures were impacted by TMD, and how to select the right TMD parameters. Further evidence of the TMD's superior ability to lessen the base-isolation subsystem's structural reaction can be found in [21]. Since the base-isolated structures' minor inter-story drifts are preserved and the base-isolation subsystem's displacement demand is lowered, TMDs have the potential to produce better control results than adding extra dampening to the isolation layer. Regarding the best selection of TMD design parameters added to base-isolation subsystems, some frequency domain analyses are reported in [20], whilst in [24], the best TMD design parameters are chosen taking into account the scenario of a white noise ground excitation for the optimal choice of the TMD properties added to the base-isolation subsystems. There aren't many studies in this area that have thought about using alternative passive control mechanisms to lessen the displacement requirement of base-isolated structures. With regard to wind-induced motion of base-isolated buildings, Particularly, a Tuned Liquid Damper case was conducted [25].

One intriguing control mechanism that has recently attracted attention in the research field is TLCD (Tuned Liquid Column Damper). It uses the same mechanical principles as the TMD to dissipate structural vibrations. The liquid surface in the U-shaped container's two vertical columns is continuously exposed to the pressure of the atmosphere. Since the liquid's theoretical natural frequency of oscillation solely varies according to how long the entire

liquid column is [26,27], TLCDs are especially appropriate for systems with a dominating initial mode having a fundamental natural frequency that is really low, such as base-isolated buildings.

The use of liquid as a source of water makes TLCD an appealing choice for vibration reduction because it is inexpensive, simple to deploy, requires little maintenance, and doesn't need to add mass to the building. Ziegler [8] is a good source for readers who want a thorough examination of the advantages that TLCDs have over other passive vibration control devices. For a semi-active TLCD, numerous on-off damping controllers have recently been implemented [28]. Ziegler put forth a brand-new TLCD for reducing vertical vibrations [29]. TLCD's efficacy depends on its equivalent damping ratio and its natural frequency optimally tuned to the parameters of the main structure. Optimal tuning parameters were derived depending on a wide range of excitation and optimization criteria [31]. The optimal parameters of TLCD can be calculated by utilizing the suggested approximation [9]. The actual TLCD design is impracticable since neither random vibration nor modern control theories can offer a comparable design representation of TMD. A parallel calculation approach of converting TLD-structure into TMD-structure was proposed by Liu et al. [33] giving explicit physical meaning with a reasonable transformation derivation process. In [34], the process for converting a TLCD-structure to a TMD-structure was used to investigate the numerical calculations, and the method of Den Hartog was used to optimize TLCD's parameters.

In this thesis, an exact optimization using metaheuristics is proposed for the optimization of TLCD positioned on base level of base-isolated structures considering properties of both base-isolators and TLCD as design variables. First, dynamic analysis of a bench mark base-isolated TLCD-controlled structure was done by generating the motion equations of the structure and the hybrid control systems and modeling these equations in Matlab with Simulink. Then, the design methodology for the hybrid system was generated via an existing metaheuristic method for optimizing BI subsystem and TLCD system specifically for base-isolated structues. The investigated metaheuristic was improved by modification according to the study's requirements. In addition, multi-cases of design constants were investigated to provide practical solutions to engineers. JAYA metaheuristic algorithm was used for designing the optimum BI and TLCD suiting systems characterized by a predominant first mode with a very low fundamental natural frequency. 44 earthquakes from the FEMA P-695

far-field set were used in time-history studies detailed in [35] was employed to examine the control performances of the hybrid control system. To be specific, the benchmark base-isolated building with 20 stories from [36] has been considered. Furthermore, numerical simulations were performed on the controled bench mark building structure by th hybrid control system, and the results were compared with the base isolated building without TLCD and the simple building without control to investigate the effectiveness of the optimized hybrid control system.

2.2. SEISMIC ISOLATION

2.2.1. Principle of Seismic Isolation

Seismic isolation aims to reduce seismic demand instead of increasing the structure's capacity. In seismically isolated systems, a flexible interface is introduced between the foundation and the base of structure to decouple the superstructure from the earthquake ground motion. Therefore, the isolation system dissipates the energy in damping and shifts the fundamental period of the structure to a large value, limiting the portion of force transferred to the superstructure. As a result, interstory drift and floor accelerations are reduced drastically. A flexible structural system from earthquake resistance view point is created by matching fundamental frequencies of base-isolated structures and predominant frequency contents of earthquakes [53].

By simultaneously reducing both floor accelerations and relative floor displacements, seismic isolation protects the structure along with its content; hence, it is accepted as an earthquake-resistant design method. Seismic isolation technology is highly preferred especially in strategic buildings where sensitive equipment is intended to be protected from hazardous effects during earthquakes such as schools, hospitals, and industrial structures [54]. Seismic isolated structures' performance is generally evaluated by the base displacements, base and floor accelerations, and relative floor displacements [42].

Although properly designed seismic isolation systems reduce floor accelerations and relative floor displacements to acceptable limits in far-fault earthquakes without causing unacceptably large displacements, the effectiveness of isolation systems in near-fault earthquakes is questionable due to its potential for very large isolator displacements [55].

2.2.2. Types of Isolation Systems

In general, seismic isolation systems are divided into two main groups: elastomeric-based systems and friction-based systems. As technology develops, different isolation systems emerge but these new systems must satisfy the following fundamental requirements [56]:

1. High capacity of lateral deformation: The isolation layer must exhibit low lateral stiffness which decreases the frequency of the base-isolated structure significantly when compared to a similar structure with a fixed base and helps to shift away the structure's frequency from severe earthquakes' dominant frequency.

2. Adequate lateral stiffness: Isolation systems must have adequate lateral rigidity to avoid small movement of the structure under low-level loads such as wind and minor earthquakes and to fulfill the serviceability conditions.

3. High vertical rigidity: To support the total weight of the structure and to avoid crashing or lateral bulging, isolation systems must have high vertical rigidity.

4. Force effect restoration: After a large displacement due to earthquake loads, a restoring force effect is necessary so the structure can return to its original position.

5. Adequate damping ratio: A damping ratio that is (15 to 30%) dissipates more energy coming from the earthquake and prevents potential resonance and high displacements of the super structure.

2.3. TUNED LIQUID COLUMN DAMPER

TLCD is a passive control device, that depends on the motion of an oscillating liquid column inside a container which counteracts external motion, while a built-in orifice plate induces turbulent damping forces that dissipate kinetic energy and structural vibrations.

2.3.1. Geometry of TLCD

Literature [57] has proposed various TLCD geometries. The container, which consists of two vertical and one horizontal pipe, is the most widely used [58]. Symmetric V-shaped TLCD is a more flexible device with arbitrary inclined pipe sections and a variable length horizontal element, Figure 1 illustrates B and H, which demonstrates the liquid columns' inclined and horizontal lengths, respectively, and where cross-sectional areas AB and AH are assumed to be constant. Therefore, 2HxAH plus BxAB make up the fluid volume. The displacement, u1 = u2 = u(t), describes the liquid column's relative motion.

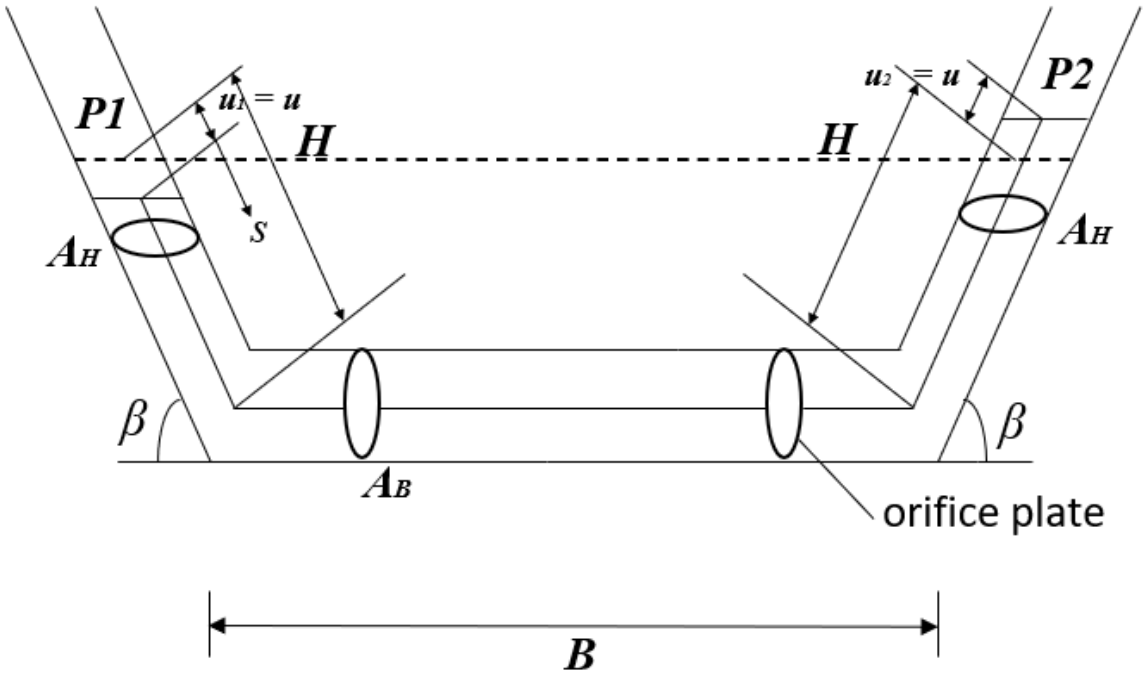

Figure 1 Tuned Liquid Column Dampr Geometry

2.3.2. The Efficacy of TLCD

The TLCD's equivalent damping ratio and natural frequency, when perfectly tuned to the characteristics of the primary structure, determines its efficacy. With an increased ratio of TLCD mass to structural mass, the dynamic amplification of the main structure is reduced. In practice, there is a maximum mass ratio of approximately 5%.

2.3.3. Advantages of TLCD

The same mechanical principle governs the efficacy of the TLCD and the tuned mass damper (TMD), although TLCD offers several benefits over TMD. [8]. To begin with, TLCD is a device with low cost since it is easy to implement in new buildings and to retrofit in existing structures, because there are no complicated mechanical components involved, tuning its frequency can be accomplished by merely varying the liquid amount. The TLCD is effective for buildings with a fundamental frequency lower than about 12.56 Rad/sec. Certainly, if a water tank is incorporated into the design of a TLCD for water supply and fire fighting, neither the cost nor the weight is increased (Fire caused by an earthquake is not taken into account.) [41].

2.3.4. Modeling of TLCD

2.3.4.1. TLCD's Equation of Motion for Reducing Single-Direction Vibration

The equation of motion is obtained by integrating along the relative streamline. The ground acceleration is provided by $\ddot{w}_g$, see Fig. 1 [32],

$$\left.\begin{aligned} \ddot{u} + \frac{\Delta p_L}{\rho L_{eff}} + \frac{\Delta p}{\rho L_{eff}} + \omega_A^2 u &= -k(\ddot{w}_{\mathrm{g}} + \ddot{w}) \\ \Delta p &= p_2 - p_1 \\ \mathrm{V}\Delta p_L &= \frac{\rho|\dot{u}|u}{2}\lambda(Re) \end{aligned}\right\} \quad (1)$$

where ρ, Δp and Δp_L designate the density of a liquid, the streamlined pressure loss and the pressure difference. Δp_L is a product of λ(Re) (loss factor), where Re = $2R\frac{\dot{u}}{\mathrm{v}}$ (Reynolds number), and the stagnation pressure $\frac{\rho|\dot{u}|u}{2}$. The kinematic viscosity is denoted by the letter v, and R is a typical cross-sectional size. The effective length L_{eff} of the liquid column and the geometry-dependent excitation influence factors k, where $\ddot{w}$ is the floor's relative horizontal displacement. All this is defined by,

$$\left.\begin{aligned} k &= \frac{\mathrm{B} + 2\mathrm{H}\cos\beta}{L_{eff}} \\ L_{eff} &= 2H + \frac{A_H}{A_B}B \end{aligned}\right\} \quad (2)$$

The TLCD's undamped linear natural circular frequency can be calculated using,

$$\omega_A = \sqrt{\frac{2gsin\beta}{L_{eff}}} \quad (3)$$

g stands for the gravitational constant, g = 9.81 m/s^2. The free surfaces' air pressure is nearly equal to the ambient pressure $p_1 = p_2 = p_0$ and the pressure differential Δp vanishes when the nonlinear damping factor $\frac{\Delta p_L}{\rho L_{eff}}$ is replaced by its viscous counterpart $2\xi_A\omega_A\dot{u}$.

Only the forces of interaction between the massless, rigid, liquid-filled system and the supporting floor are considered, assuming that the dead weight of rigid piping has increased the floor mass (at this point, dead fluid mass is not considered.). The following are the reaction forces affecting the supporting floor,

$$\left.\begin{aligned} F_x &= -m_f(\ddot{w}_g + \bar{k}\ddot{u}) \\ \bar{k} &= kL_{eff}/L_1 \\ L_1 &= 2H + \frac{A_B}{A_H}B \end{aligned}\right\} \quad (4)$$

where $m_f = \rho A_H L_1$ designates the total fluid mass.

2.3.4.2. TLCD's Equation of Motion for Reducing Coupled Translation and Rotation Vibrations

When a TLCD is implemented, its direction in the floor of an asymmetrical structure is directed by the reference point A($y_A, z_A, 0$) and the angle γ reference to the direction of y. The generalized nonstationary method, the Bernoulli equation , is used to construct the optimal fluid flow equation for rigid pipe systems, check Figure 2 [32],

$$\ddot{u} + 2\xi_A\omega_A\dot{u} + \omega_A^2 u$$

$$= -k\{[\ddot{v}_g + \ddot{v} - (z_A - z_{C_M})\ddot{\theta}]\cos\gamma + [\ddot{w}_g + \ddot{w} + (y_A - y_{C_M})\ddot{\theta}]\sin\gamma\} \quad (5)$$

In Y, Z, and θ directions, The control forces F_{Ay}, F_{AZ} and M_A are determined by using the momentum and angular momentum of the moving fluid,

$$\left.\begin{aligned} F_{Ay} &= m_f[\ddot{v}_g + \ddot{v} - (z_A - z_{C_M})\ddot{u}_T/r_S] + \bar{k}m_f\ddot{u}\cos\gamma \\ F_{Az} &= m_f[\ddot{w}_g + \ddot{w} - (y_A - y_{C_M})\ddot{u}_T/r_S] + \bar{k}m_f\ddot{u}\sin\gamma \\ u_T &= \theta r_S \\ M_{Ax} &= m_f\bar{k}_3H^2\ddot{\theta} \\ \bar{k}_3 &= \frac{2H}{L_1}\left[\left(\frac{B}{2H}\right)^2 + \frac{A_B}{3A_H}\left(\frac{B}{2H}\right)^3 + \frac{B}{2H}\cos\beta + \frac{1}{3}\cos^2\beta\right] \end{aligned}\right\} \quad (6)$$

Linearized moment Mx can be calculated from,

$$M_x = M_{Ax} - F_{Ay}(z_A - z_M) + F_{Az}(y_A - y_M) \quad (7)$$

2.4. APPROXIMATE SUBSTRUCTURE SYNTHESIS

Recently, there has been an increasing interest to apply TLCDs as a solution for the vibration reduction of structures [30]. The impact of TLCD's damping on controlling structural vibrations depends on damping value and proper tuning. Taking advantage of the proposed approximated formulation in [9], the ideal TLCD parameters can be calculated by a smooth function that can be formed and easily minimized and defines the primary system variance. However, the design of the real TLCD is cumbersome. The TLCD damping effect simulation in MATLAB for a non-standard structure is too complicated. An equivalent computation approach was put out by [33], providing a plausible process of transformation of a TLD with a clear physical meaning (TMD-structure to TLD-structure system). The approach of converting the TLCD-structure into the TMD-structure was utilized in [34] to examine parameter optimization and numerical calculation, and the method of Den Hartog was

employed for optimizing the TLCD. In this thesis and proceeding from the method of transformation used in [34], an optimization method was developed and a computer code was written based on dynamic analysis of the structure and metaheuristic optimization methods in order to come out with an optimum design for the TLCD and BI systems.

2.4.1. TLCD/TMD in Symmetric Structure

For an implemented TLCD on a floor that is propelled by ground motions $\overrightarrow{\ddot{\mathrm{w}}_{\mathrm{g}}}$ and loads of wind $\vec{\mathrm{F}}(t)$, the following equation of motion determines how the TLCD and the main structure interact,

$$\left.\begin{aligned} \widetilde{M}\overrightarrow{\ddot{\mathrm{w}}} + \tilde{C}\overrightarrow{\dot{w}} + \widetilde{K}\overrightarrow{\mathrm{w}} &= -\widetilde{M}\overrightarrow{\ddot{\mathrm{w}}_{\mathrm{g}}} + \vec{\mathrm{F}}(t) + \vec{\mathrm{s}}F_z \\ \vec{\mathrm{s}} &= [0, \dots, 1, \dots, 0] \end{aligned}\right\} \quad (8)$$

$F_z = -m_f(\ddot{\mathrm{w}}_{\mathrm{g}} + \vec{\mathrm{s}}^T\overrightarrow{\ddot{\mathrm{w}}} + \bar{k}\ddot{u})$, where $\widetilde{M}$ is the diagonal mass matrix, where each floor has three lumped mass elements. The primary system's light damping and stiffness matrices are $\tilde{C}$ and $\widetilde{K}$, respectively. Expanding the floor displacement $\overrightarrow{\mathrm{w}}$ to a modal series, the formula becomes, $\overrightarrow{\mathrm{w}} = \sum_{i=1}^{n} q_i\overrightarrow{\phi_i}$. By substituting it in the left side of equation no. (8), then it decouples by pre-multiplication with the transposed ortho-normalized modal vector $\overrightarrow{\phi_i}^T$ and divided by modal mass m_j, the matrix form of the coupled system of linearized equation results,

$$\begin{bmatrix} 1+\mu_j & \dfrac{\bar{k}_j\mu_j}{\varphi_{ji}} \\ \varphi_{ji}k_j & 1 \end{bmatrix}\begin{bmatrix}\ddot{\mathrm{q}}_{\mathrm{j}} \\ \ddot{\mathrm{u}}_{\mathrm{j}}\end{bmatrix} + \begin{bmatrix} 2\xi_{sj}\omega_{sj} & 0 \\ 0 & 2\xi_{Aj}\omega_{Aj}\end{bmatrix}\begin{bmatrix}\dot{\mathrm{q}}_{\mathrm{j}} \\ \dot{\mathrm{u}}_{\mathrm{j}}\end{bmatrix} + \begin{bmatrix} {\omega^2}_{sj} & 0 \\ 0 & {\omega^2}_{Aj}\end{bmatrix}\begin{bmatrix}q_{\mathrm{j}} \\ u_{\mathrm{j}}\end{bmatrix} =$$

$$-\begin{bmatrix}\xi_j \\ k_{\mathrm{j}}\end{bmatrix}\ddot{\mathrm{w}}_{\mathrm{g}} + \begin{bmatrix}\mathrm{f}_j \\ 0\end{bmatrix}$$

$$\xi_j = \frac{\overrightarrow{\varphi_j}^T\widetilde{M}rs + \varphi_{ji}m_{fj}}{\overrightarrow{\varphi_j}^T\widetilde{M}\overrightarrow{\varphi_j}},\ \mu_j = \frac{{\varphi^2}_{ji}m_{fj}}{\overrightarrow{\varphi_j}^T\widetilde{M}\overrightarrow{\varphi_j}},\ \mathrm{f}_j = \frac{\overrightarrow{\varphi_j}\vec{\mathrm{F}}(t)}{\overrightarrow{\varphi_j}^T\widetilde{M}\overrightarrow{\varphi_j}},\ {\omega^2}_s = \frac{\overrightarrow{\varphi_j}^T\widetilde{K}\overrightarrow{\varphi_j}}{\overrightarrow{\varphi_j}^T\widetilde{M}\overrightarrow{\varphi_j}}$$

$$2\xi_s\omega_s = \frac{\overrightarrow{\varphi_j}^T\tilde{C}\overrightarrow{\varphi_j}}{\overrightarrow{\varphi_j}^T\widetilde{M}\overrightarrow{\phi_j}}$$

where μ_j, ξ_{sj}, ω_{sj} and ω_{Aj} are, respectively, the mass ratio, the modal structural damping ($\xi_{sj} \ll 1$), the main structure's circular natural frequency, and TLCD's circular natural frequency. The primary system is changed when the equivalent-TMD is used in place of the TLCD; the parameters are indicated by an asterisk,

$$\left.\begin{array}{c} \widetilde{M}^*\ddot{\overrightarrow{w}} + \tilde{C}^*\overrightarrow{w} + \widetilde{K}^*\overrightarrow{w} = -\widetilde{M}^* r_s \ddot{\overrightarrow{w}}_g + \vec{F}(t) + \vec{s}F^*_z \\ \text{Control force: } F^*_z = -m^*_A(\ddot{w}_g + \vec{s}^T\ddot{\overrightarrow{w}} + \ddot{u}^*) \end{array}\right\} \quad (10)$$

$$\ddot{u}^* + 2\xi_A{}^*\omega_A{}^*\dot{u}^* + \omega_A{}^{*2}u^* = -(\ddot{w}_g + \vec{s}^T\ddot{\overrightarrow{w}}) \quad (11)$$

The matrix form of the TMD-structure interaction equation is obtained by combining Equations (10) and (11).

$$\left.\begin{array}{c} \begin{bmatrix} 1+\mu^*_j & \mu^*_j \\ 1 & 1 \end{bmatrix}\begin{bmatrix} \ddot{q}_j \\ \ddot{u}^*_j \end{bmatrix} + \begin{bmatrix} 2\xi^*_{sj}\omega^*_{sj} & 0 \\ 0 & 2\xi^*_{Aj}\omega^*_{Aj} \end{bmatrix}\begin{bmatrix} \dot{q}_j \\ \dot{u}^*_j \end{bmatrix} + \begin{bmatrix} \omega^{*2}_{sj} & 0 \\ 0 & \omega^{*2}_{Aj} \end{bmatrix}\begin{bmatrix} q_j \\ u^*_j \end{bmatrix} \\ = -\begin{bmatrix} \xi^*_j \\ 1 \end{bmatrix}\ddot{w}_g + \begin{bmatrix} f^*_j \\ 0 \end{bmatrix} \\ \xi^*_j = \frac{\overrightarrow{\varphi_j}^T\widetilde{M}^* r s + \varphi_{ji} m_{Aj}}{\overrightarrow{\varphi_j}^T\widetilde{M}^*\overrightarrow{\varphi_j}},\ \mu^*_j = \frac{\varphi^2_{ji} m_{Aj}}{\overrightarrow{\varphi_j}^T\widetilde{M}^*\overrightarrow{\varphi_j}},\ f^*_j = \frac{\overrightarrow{\varphi_j}\vec{F}(t)}{\overrightarrow{\varphi_j}^T\widetilde{M}^*\overrightarrow{\varphi_j}},\ \omega^{*2}_s = \frac{\overrightarrow{\varphi_j}^T\widetilde{K}^*\overrightarrow{\varphi_j}}{\overrightarrow{\varphi_j}^T\widetilde{M}^*\overrightarrow{\varphi_j}} \\ 2\xi^*_s\omega^*_s = \frac{\overrightarrow{\varphi_j}^T\widetilde{C}^*\overrightarrow{\varphi_j}}{\overrightarrow{\varphi_j}^T\widetilde{M}^*\overrightarrow{\phi_j}} \end{array}\right\} \quad (12)$$

Where, in turn, μ^*_j, ω^*_{sj}, and ω^*_{Aj} stand for the alternative mass ratio, the circular natural frequency of the equivalent structure and the circular natural frequency of the equivalent TMD.

2.4.2. TLCD/TMD in Asymmetric Structure

On the i-th level of an N-story plan-asymmetric space frame, a single TLCD is installed with γ angle reference to the direction of y and A($y_A, z_A, 0$) as a reference point. The equation of motion for the building, using an oblique point excitation, can be written as a hypermatrix, $\ddot{\overrightarrow{x}}_g^T = [\ddot{v}_g\ \ddot{w}_g\ 0]$and by wind forces $\vec{F}(t)$,

$$\left.\begin{gathered}\widetilde{M}\ddot{\vec{\mathrm{x}}}+\tilde{C}\dot{\vec{x}}+\widetilde{K}\vec{\mathrm{x}}=-\widetilde{M}\ddot{\overrightarrow{\mathrm{x}_{\mathrm{gN}}}}+\vec{\mathrm{F}}(t)+\vec{F_A},\ \vec{\mathrm{x}}^T=[\vec{x_1}^T\ldots\vec{x_i}^T\ldots\vec{x_N}^T],\\ \vec{x_i}^T=[v_{\mathrm{i}}\ w_{\mathrm{i}}\ u_{\mathrm{Ti}}],\ u_{\mathrm{Ti}}=\theta_i\ r_{Si},\ \ddot{\overrightarrow{\mathrm{x}_{\mathrm{gN}}}}=\tilde{E}_N\ddot{\vec{\mathrm{x}}}_{\mathrm{g}},\\ \tilde{E}_N=\begin{bmatrix}1&0&0&1&0&0&1&\ldots\\0&1&0&0&1&0&0&\ldots\\0&0&0&0&0&0&0&\ldots\end{bmatrix}^T,\ \widetilde{M}=diag[\widetilde{M}_1\quad\ldots\widetilde{M}_i\quad\ldots\widetilde{M}_N]=3N\times3N,\\ \vec{F_A}^T=\left[0,\quad\ldots,\ F_{Aiy},\ F_{Aiz},\frac{M_{xi}}{r_{si}},\quad\ldots,0\right]\end{gathered}\right\}\quad(13)$$

Isolated modal displacements $v_{\mathrm{i}}=q_j\phi_{j(3i-2)}$, $w_{\mathrm{i}}=q_j\phi_{j(3i-1)}$, $u_{\mathrm{Ti}}=\theta_i\,r_{Si}=q_j\phi_{j3i}$ are substituted in the right side of the equation of TLCD and the control forces. The main system's linearized coupled system of modal equations with attached TLCD is represented in matrix form as,

$$\left.\begin{gathered}\begin{bmatrix}1+\mu_j&\dfrac{\bar{k}_j\lambda_j\mathrm{m}_{fj}}{m_j}\\ k_j\lambda_j&1\end{bmatrix}\begin{bmatrix}\ddot{\mathrm{q}}_{\mathrm{j}}\\ \ddot{\mathrm{u}}_{\mathrm{j}}\end{bmatrix}+\begin{bmatrix}2\xi_{sj}\omega_{sj}&0\\0&2\xi_{Aj}\omega_{Aj}\end{bmatrix}\begin{bmatrix}\dot{\mathrm{q}}_{\mathrm{j}}\\ \dot{\mathrm{u}}_{\mathrm{j}}\end{bmatrix}+\begin{bmatrix}{\omega^2}_{sj}&0\\0&{\omega^2}_{Aj}\end{bmatrix}\begin{bmatrix}q_{\mathrm{j}}\\ u_{\mathrm{j}}\end{bmatrix}\\ =-\begin{bmatrix}\vec{L_J}^T/m_{\mathrm{j}}\\ k_{\mathrm{j}}\vec{r_s}^T\end{bmatrix}\ddot{\overrightarrow{\mathrm{x}_{\mathrm{g}}}}+\begin{bmatrix}\vec{\phi_J}^T\vec{\mathrm{F}}(t)/m_{\mathrm{j}}\\0\end{bmatrix}\end{gathered}\right\}\quad(14)$$

$$\left.\begin{gathered}\lambda_j=\mathrm{v}_{ij}cos\gamma+\mathrm{w}_{ij}sin\gamma,\ \mu_j=\frac{m_{fj}{V^2}_j}{m_j}<6\%,\ {V^2}_j={V^*_j}^2+\bar{k}_1(\phi_{j3i}H/\,r_{si})^2,\\ \vec{\mathrm{r}}_s^{\,T}=[cos\gamma\ \sin\gamma\ 0],\ {V^*_j}^2=V^2{}_{Aij}+w^2{}_{Aij},\ \mathrm{v}_{Aij}=\phi_{j(3i-2)}-\phi_{j3i}(\mathrm{z}_{Aij}-\mathrm{z}_{C_{Mi}})/\,r_{si},\\ \vec{\mathrm{L}}_j^{\,T}=[\mathrm{L}_{jy}\ \ \mathrm{L}_{jz}\ \ 0],\ \bar{k}_1=\frac{2H}{\mathrm{L}_1}\left[\left(\frac{B}{2\mathrm{H}}\right)^2+\frac{\mathrm{A}_B}{3\mathrm{A}_H}\left(\frac{B}{2\mathrm{H}}\right)^3+\frac{B}{2\mathrm{H}}cos\beta+\frac{1}{3}cos^2\beta\right],\\ \mathrm{w}_{Aij}=\phi_{j(3i-1)}+\phi_{j3i}(\mathrm{y}_{Aij}-\mathrm{y}_{C_{Mi}})/\,r_{si},\ \mathrm{L}_{jy}=\sum_{n=1}^{N}m_{Sn}\phi_{j(3n-2)}+m_{fj}\mathrm{v}_{Aij},\end{gathered}\right\}\quad(15)$$

$$\mathrm{L}_{jz} = \sum_{n=1}^{N} m_{Sn}\phi_{j(3n-1)} + m_{fj}\mathrm{w}_{Aj}$$

Eq. (16) is produced by the standard analysis when the passive spring-mass damper is taken into account in the same location on the same floor connected. To refer to TMD, an asterisk is used to indicate every parameter,

$$\left.\begin{aligned} \widetilde{M}^{*}\ddot{\vec{\mathrm{x}}} + \widetilde{K}^{*}\vec{\mathrm{x}} &= -\widetilde{M}^{*}\ddot{\vec{\mathrm{x}}}_{\mathrm{gN}} + \vec{\mathrm{F}}(t) + \vec{F_A}^{*}, \\ \widetilde{M}^{*} &= diag\left[\widetilde{M}^{*}{}_{1} \ldots \widetilde{M}^{*}{}_{i} \ldots \widetilde{M}^{*}{}_{N}\right] = 3N \times 3N, \\ \vec{F_A}^{*T} &= \left[0, \ldots, F^{*}{}_{Aiy}, F^{*}{}_{Aiz}, M^{*}{}_{xi}/\, r_{Si} \ldots, 0\right], \\ F^{*}{}_{Aiy} &= m^{*}{}_{A}\left[\ddot{\mathrm{v}}_{\mathrm{g}} + \ddot{\mathrm{v}}_{\mathrm{i}} - \left(z_{Ai} - z_{C_{Mi}}\right)\ddot{\theta}_{\mathrm{i}}\right] + m^{*}{}_{A}\ddot{u}^{*}cos\gamma \\ F^{*}{}_{Aiz} &= m^{*}{}_{A}\left[\ddot{\mathrm{w}}_{\mathrm{g}} + \ddot{\mathrm{w}}_{\mathrm{i}} - \left(y_{Ai} - y_{C_{Mi}}\right)\ddot{\theta}_{\mathrm{i}}\right] + m^{*}{}_{A}\ddot{u}^{*}sin\gamma,\ M^{*}{}_{Aix} \approx 0 \end{aligned}\right\} \quad (16)$$

The ith story's approximated linearized equation of motion for TMD is,

$$\ddot{u}^{*} + 2\xi^{*}{}_{A}\omega^{*}{}_{A}\dot{u}^{*} + \omega^{2}{}_{A}\mathrm{u}^{*}$$

$$= -\left[\ddot{\mathrm{v}}_{\mathrm{g}} + \ddot{\mathrm{v}}_{\mathrm{i}} - \left(z_{Ai} - z_{C_{Mi}}\right)\ddot{\theta}_{\mathrm{i}}\right]cos\gamma - \left[\ddot{\mathrm{w}}_{\mathrm{g}} + \ddot{\mathrm{w}}_{\mathrm{i}} - \left(y_{Ai} - y_{C_{Mi}}\right)\ddot{\theta}_{\mathrm{i}}\right]sin\gamma \quad (17)$$

Taking into account the MDOF structure with the TMD, the coupled system's approximated modal matrix equation of motion becomes,

$$\begin{bmatrix} 1+\mu^{*}{}_{j} & \dfrac{\lambda_j \mathrm{m}^{*}{}_{Aj}}{m^{*}{}_{j}} \\ \lambda_j & 1 \end{bmatrix}\begin{bmatrix}\ddot{\mathrm{q}}_{\mathrm{j}} \\ \ddot{\mathrm{u}}_{\mathrm{j}}\end{bmatrix} + \begin{bmatrix} 2\xi^{*}{}_{Sj}\omega^{*}{}_{Sj} & 0 \\ 0 & 2\xi^{*}{}_{Aj}\omega^{*}{}_{Aj}\end{bmatrix}\begin{bmatrix}\dot{\mathrm{q}}_{\mathrm{j}} \\ \dot{\mathrm{u}}^{*}{}_{\mathrm{j}}\end{bmatrix} + \begin{bmatrix}\omega^{*2}{}_{sj} & 0 \\ 0 & \omega^{*2}{}_{Aj}\end{bmatrix}\begin{bmatrix} q_{\mathrm{j}} \\ u^{*}{}_{\mathrm{j}}\end{bmatrix}$$

$$= -\begin{bmatrix}\overrightarrow{L^{*}_{J}}^{T}/m^{*}{}_{\mathrm{j}} \\ \vec{r}_{S}^{\,T}\end{bmatrix}\ddot{\vec{\mathrm{x}}}_{\mathrm{g}} + \begin{bmatrix}\overrightarrow{\phi_J}^{T}\vec{\mathrm{F}}(t)/m^{*}{}_{\mathrm{j}} \\ 0\end{bmatrix} \quad (18)$$

$$\left.\begin{aligned} \mu^*_j &= m^*_{\mathrm{A}j} V^{*2}_j / m^*_{\mathrm{j}} \\ \overrightarrow{L^*_J}^T &= [L^*_{jy} \quad L^*_{jz}] \\ L^*_{jy} &= \sum_{n=1}^{N} m^*_{Sn} \phi_{j(3n-2)} + m^*_{Aj} \mathrm{v}_{Aij} \\ L^*_{jz} &= \sum_{n=1}^{N} m^*_{Sn} \phi_{j(3n-1)} + m^*_{Aj} \mathrm{w}_{Aij} \end{aligned}\right\} \quad (19)$$

m_{Sn}, m^*_{Sn} and m_j, m^*_{j} denote the mass of the floor number n and the modal mass. The modified participation factor $\overrightarrow{L_J}$, $\overrightarrow{L^*_J}$ and the effective wind load $\overrightarrow{\phi_J}^T \vec{\mathrm{F}}(t)/m_{\mathrm{j}}$, $\overrightarrow{\phi_J}^T \vec{\mathrm{F}}(t)/m^*_{\mathrm{j}}$ are identified. v_{Aij} and w_{Aij} denote the reference point A_i's modal displacements in y- and z-directions, respectively. $m_f(1 - k\bar{k})$ must be regarded as the dead fluid mass, which reduces the natural frequency of the main structure slightly.

3. METHOD

This study aims to find the optimum design for the passive hybrid control system to reduce displacements and protect the base isolators by implementing isolators and TLCD device on the base level of the structure. In this study, metaheuristics methods will be used to establish the optimum design variables of base-isolators (stiffness and damping) and TLCD (shape properties to tune stiffness and damping). In this context, a benchmark model of a twenty-story base-isolated building is used. Details of the building are explained in a sub-sequent section.

3.1. MODAL TUNING OF TLCD

When the modes of the structure are well determined, the coupled TLCD-structure is still an approximation. Metaheuristic algorithms could carry out the TLCD's modal tuning through similarity between equivalent TLCD and TMD.

3.1.1. Similarity between TLCD and TMD when Used in Symmetric Structure

Defining the connection for both u and u* is the first step. The right side of the second equations in Equations (1) and (11), when compared, reveal that the same excitation is proportional.

$$u^*=u/k_j \tag{20}$$

Equations (9) and (12)'s left side of the second equation can be substituted for this result to produce the following,

$$\omega^*_{Aj} = \omega_{Aj}, \xi^*_{Aj} = \xi_{Aj} \tag{21}$$

By adding these outcomes to the first equation in Eqs. (9) and (11),

$$\left.\begin{aligned} \frac{\mu_j \overline{k_j}}{1+\mu_j} &= \frac{\mu^*_j}{k_j(1+\mu^*_j)} \\ \frac{1}{1+\mu_j}\omega^2_{sj} &= \frac{1}{1+\mu^*_j}\omega^{*2}_{sj} \\ \frac{1}{1+\mu_j}2\xi_{sj}\omega_{sj} &= \frac{1}{1+\mu^*_j}2\xi^*_{sj}\omega^*_{sj} \\ \frac{1}{\varphi_j{}^T\widetilde{M}\varphi_j(1+\mu_j)} &= \frac{1}{\varphi_j{}^T\widetilde{M^*}\varphi_j(1+\mu^*_j)} \end{aligned}\right\} \quad (22)$$

and as a result, the analogous TMD-main system's mass ratio changes into,

$$\left.\begin{aligned} \mu^*_j &= \frac{\mu_j k_j \overline{k_j}}{1+\mu_j(1-k_j\overline{k_j})} < \mu_j \\ \delta_{jopt} &= \frac{\omega_{Ajopt}}{\omega_{sj}} = \frac{\delta_{jopt}{}^*}{\sqrt{1+\mu_j\left(1-k_j\overline{k_j}\right)}} \\ \omega^*_{sj} &= \frac{\omega_{sj}}{\sqrt{1+\mu_j\left(1-k_j\overline{k_j}\right)}} < \omega_{sj} \\ \xi^*_{sj} &= \frac{\xi_{sj}}{\sqrt{1+\mu_j\left(1-k_j\overline{k_j}\right)}} < \xi_{sj} \end{aligned}\right\} \quad (23)$$

And

$$\left.\begin{aligned} m^*_j &= m_j\left(1+\mu_j\left(1-k_j\overline{k_j}\right)\right) > m_j \\ m_{Aj} &= k_j\overline{k_j}\, m_{fj} < m_{fj} \end{aligned}\right\} \quad (24)$$

The TLCD's dead fluid mass is part of the correlated structural mass, $m_f\left(1 - k\,\bar{k}\right)$.

3.1.2. Similarity between TLCD and TMD when Used in Asymmetric Structure

The fundamental framework for utilizing the results of the TMD design is the similarity between TLCD and TMD coupled with a multi-degree-of-freedom symmetric structure. Later, the method for a larger class of asymmetric structures with coupled TLCD has been researched, and the findings are helpfully summarized. The TMD-main system's modal mass ratio is given by,

$$\boldsymbol{\mu^*_j = \mu_j \frac{k_j \bar{k_j} (V^*_j / V_j)^2}{1 + \mu_j (1 - k_j \bar{k_j} (V^*_j / V_j)^2)} < \mu_j} \tag{25}$$

and the modified main system's frequency and damping ratio with an equivalent TMD are,

$$\left.\begin{aligned} \omega^*_{Sj} &= \frac{\omega_{Sj}}{\sqrt{1 + \mu_j (1 - k_j \bar{k_J} (V^*_j / V_j)^2)}} < \omega_{Sj} \\ \xi^*_{Sj} &= \frac{\xi_{Sj}}{\sqrt{1 + \mu_j \left(1 - k_j \bar{k_J} (V^*_j / V_j)^2\right)}} < \xi_{Sj} \end{aligned}\right\} \tag{26}$$

The TMD frequency ratio $\delta^*_{jopt} = \frac{\omega^*_{Ajopt}}{\omega^*_{Sj}}$ and the TLCD frequency ratio $\delta_{jopt} = \frac{\omega_{Ajopt}}{\omega_{Sj}}$ are therefore linked by the general transformation,

$$\delta_{jopt} = \frac{\delta^*_{jopt}}{\sqrt{1 + \mu_j \left(1 - k_j \bar{k_J} (V^*_{ij} / V_{ij})^2\right)}} < \delta^*_{jopt} \tag{27}$$

This results in a slightly lower ideal frequency ratio δ_{jopt} for the TLCD than for an equivalent TMD. The ideal damping coefficient does not vary $\xi_{Ajopt} = \xi^*_{Ajopt}$. Since the dead fluid mass that appears in the denominator of Equations (25) through (27) alters the primary system, written as,

$$1 + \mu_{\,j}\left(1 - k_j\bar{k_J}\left(\frac{V^*_{ij}}{V_{\,ij}}\right)^2\right) = m_{fj}\left(1 - (k_j V^*_{ij}/V_{\,ij})^2\right) \qquad (28)$$

$$for\ k_j = \bar{k_J}\ and\ m_{\,j} = 1$$

The higher value of the geometry factor j must be attained while remaining inside the boundaries of the liquid column in order to minimize the former. Hmax|u| ≤ 2/3H [59].

3.1.3. The Metaheuristic Algorithm-Based Optimization

This section describes the structural control system's metaheuristic algorithm-based optimization approach. The optimization process's general methodology is depended on producing solutions and identifying the ideal solution by altering current solutions in accordance with the optimization's goal. In light of how this process functions, optimization can be summed up in the following 5 steps:

Step 1: The population number (pn), the user-specified algorithmic parameters, the design constants, the lower and upper bounds of the design variable, and the stopping criteria of the optimization problem are all defined. The maximum iteration number defines the stopping criteria in this chapter.

Step 2: As demonstrated in Eq. (29), a value is generated at random for each design variable that falls within its lower and upper bounds. Up until the population number specified in Step 1 is given this process is repeated.

$$X_{i,j} = X_{i(\text{low})} + rand \cdot (X_{i(\text{up})} - X_{i(\text{low})}) \qquad (29)$$

The numbers i and j in Eq. (30) stand for the number of design variables and solution vectors, respectively. Xi,j, Xi(low) and Xi(up) state the design variable's value, its lower and higher limitations, respectively. The "Rand" command, produces random numbers between 0 and 1. Following that, the generated values are kept in an initial solution matrix like the CL matrix in Eq (30),

$$CL=\begin{bmatrix} X_{1,1} & X_{1,2} & \cdots & X_{1,pn} \\ X_{2,1} & X_{2,2} & \cdots & X_{2,pn} \\ \vdots & \vdots & \cdots & \vdots \\ X_{N-1,1} & X_{N-1,2} & \cdots & X_{N,pn} \\ X_{N,1} & X_{N,2} & \cdots & X_{N-1,pn} \end{bmatrix} \quad (30)$$

Values of the design variables are represented by a potential solution vector in each column of the CL matrix. In the matrix, there are pn solution vectors and N design variables.

Step 3: The optimization problem's design constraints (limitation of control system movements) are examined, and the objective function is calculated for each solution vector. If a solution vector does not provide a design constraint, the associated solution's objective function is provided as a penalized value. The reduction of structural response is the objective function. Many cases will be considered in the study since displacement and acceleration may show different behavior for base-isolated structures.

Step 4: A new solution matrix is created with new solutions in this step. This stage is particular to the type of algorithm since the generation is carried out in accordance with the algorithm principles.

In this research, JAYA metaheuristic algorithm will be tested and modified to find the best performance. The algorithm is shortly presented in this section.

In the optimization process performed with JAYA algorithm, new solutions are created by using the already existing design variables in the initial solution matrix by applying the JAYA algorithm equation Eq. (31). Explaining details of this equation are presented in Table 1.

$$X_{i,new} = X_{i,j} + rand()\left(X_{i,g\ best} - \left|X_{i,j}\right|\right) - rand()(X_{i,g\ worst} - |X_{i,j}|) \quad (31)$$

Table 1: JAYA Optimization Components

	Variable	Description
Optimization Components	$X_{i,new}$	New value for the design variable i
	$X_{i,j}$	The design variable value for the candidate solution j in the initial matrix
	Xi, g_{best}	The best solution value for the design variable i in terms of objective function
	Xi, g_{worst}	The worst solution value for the design variable i in terms of objective function

Step 5: The final step compares the new solution matrix to the current (old) solution matrix. The old solution matrix is updated if the new solutions' objective functions outperform the current ones.

Up until the maximum iteration number, which is the stopping criteria, is given, steps 4 and 5 are repeated.

In this thesis, the code will be generated with Matlab and the dynamic analysis with structural control will be integrated via MATLAB SIMULINK.

4. RESULTS

A twenty-story shear-beam-type building (n = 20) is considered in this investigation. Each story unit's structural characteristics are as the following: m_i = each floor's mass = 300 tons; k_i = each floor's elastic stiffness = 10^6 kN/m; and C_i = each floor's inner damping coefficient = 2261 kN.sec/m (corresponding to a damping ratio of the first mode ζ_1 = 0.005), and height of each story h_i = 3 m. The computed natural frequencies for the building are 4.4, 13.2, 22, 30.6, 39, 47.2, ..., 112.4, 114.1 and 115.1 rad/sec.

The structure's control reactions are examined for three scenarios using time-history analyses with selected recorded ground excitations: the simple building without control, the base-isolated building with and without attached TLCD device. Results are based on 44 far-field ground motions. These motions are part of the FEMA P-695-FF set which is described in [35].

With the aforementioned structure and the 44 ground motions previously mentioned excitations, all response quantities' time histories have been calculated. Within 60 seconds of the earthquake episodes, maximum displacement, maximum total acceleration and maximum inter-story drift of roof level under four earthquake effects as examples are shown in Table 2. Under such strong earthquakes, all response quantities of the structure without control are big.

A rubber bearing isolation was used to lessen structural response, Figure 2(a). The base isolation subsystem's mass is m_b = 300 tons. The response of base-isolation subsystem is presumpted as linear. JAYA algorithm with three different cases was utilized to optimize the damping ratio and period of base-isolation subsystem. One case with 40 cm maximum displacement and 40% maximum damping ratio of base-isolation subsystem, another case with 40 cm maximum displacement and 20% maximum damping ratio, and the last case with 35 cm maximum displacement and 20% maximum damping ratio. The optimized properties of the base-isolation subsystem are shown in Table 3.

Table 2: Examples of The Structural Responses of Base and Roof Levels

Maximum Limitation of Base Isolation's Displacement			40 cm				35 cm			
Maximum Limitation of Base Isolation's Damping Ratio			40%		20%		20%			
Earthquake no.			21		9		37		38	
Structural Response		**Units**	**Base**	**Roof**	**Base**	**Roof**	**Base**	**Roof**	**Base**	**Roof**
Displacement	*without control*	cm	-	57.3	-	23.3	-	49.3	-	29.8
	with BI	cm	11.549	16.73	15	22.8	25.7	42	35.7	59.2
	with BI & TLCD	cm	11.547	16.72	14.9	22.6	24.7	40	35	58.6
	Reduction Value of Hybrid Control	cm	0.002	40.6	0.1	0.7	1	9.3	0.7	N/A
	Reduction Ratio	%	0.02	70.8	1.3	3	3.9	18.9	2	N/A
Total Acceleration	*without control*	m/s2	-	12.4	-	7	-	10.4	-	8.6
	with BI	m/s2	1.09	1.49	1.3	1.47	2.63	3	2.9	4.37
	with BI & TLCD	m/s2	1.10	1.50	1.28	1.49	2.56	2.9	3	4.38
	Reduction Value of Hybrid Control	m/s2	N/A	11	0.02	5.5	0.07	7.5	N/A	4.2
	Reduction Ratio	%	N/A	88	1.5	78.7	2.7	72.1	N/A	49.2
Interstory Drift	*without control*	mm	-	3.7	-	2.1	-	3.1	-	2.6
	with BI	Mm	5.3	0.448	6.73	0.44	14.9	0.90	21	1.312
	with BI & TLCD	Mm	5.4	0.45	6.72	0.45	14.6	0.88	21.2	1.313
	Reduction Value of Hybrid Control	Mm	N/A	3.3	0.002	1.6	0.3	2.2	N/A	1.3
	Reduction Ratio	%	N/A	88	0.03	78.7	2	71.8	N/A	49.2

With such an optimized base isolation subsystem, the fundamental natural frequencies of the three optimized cases became w_1 = 2.28, w_2 = 2.31 and w_3 = 2.58 rad/sec.

Within 60 seconds of the earthquake episodes, the maximum displacement, maximum total acceleration and maximum inter-story drift of roof and base levels under the same four earthquakes are shown in Table 2.

Table 3: Properties of Optimized Base-Isolated Subsystem

Case no.			1	2	3
Maximum Limitation of Base Isolation's Displacement			40 cm		35 cm
Maximum Limitation of Base Isolation's Damping Ratio			40%	20%	20%
Controller Type	**Parameters**	**Units**	**Optimum Values**		
Base Isolation	*Cb*	%	20.85	19.29	19.82
	Tb	sec	2.42	2.38	2.06

A TLCD was coupled to the base isolation subsystem to safeguard its integrity and safety. This connection is shown in Figure 2(b). The characteristics of this TLCD were optimized by using JAYA algorithm specifically for the investigated base-isolated building in order to guarantee the best response of the structure under earthquakes effects. The optimized TLCD properties for three different cases are shown in Table 4.

By using a control system of this type, the maximum displacement, maximum total acceleration and maximum interstory drift of top and base levels within 60 seconds of the same four earthquakes episodes are presented in Table 2.

The interstory drift, displacement, and total acceleration of the base-isolation subsystem as well as all floors have been estimated for the simple uncontrolled building, base-isolated building and TLCD controlled base-isolated building, for all of the FEMA P-695-FF 44 records. In this regard, Figure 3 and Figure 4 show comparison of the profile of maximum responses of the simple uncontrolled building (red line), the base-isolated building with (green line) and without (blue line) TLCD under earthquakes no. 37 and 21, respectively. Further, the maximum structural responses of base and roof levels for the hybrid controled structure are summarized in Table 5.

(a)

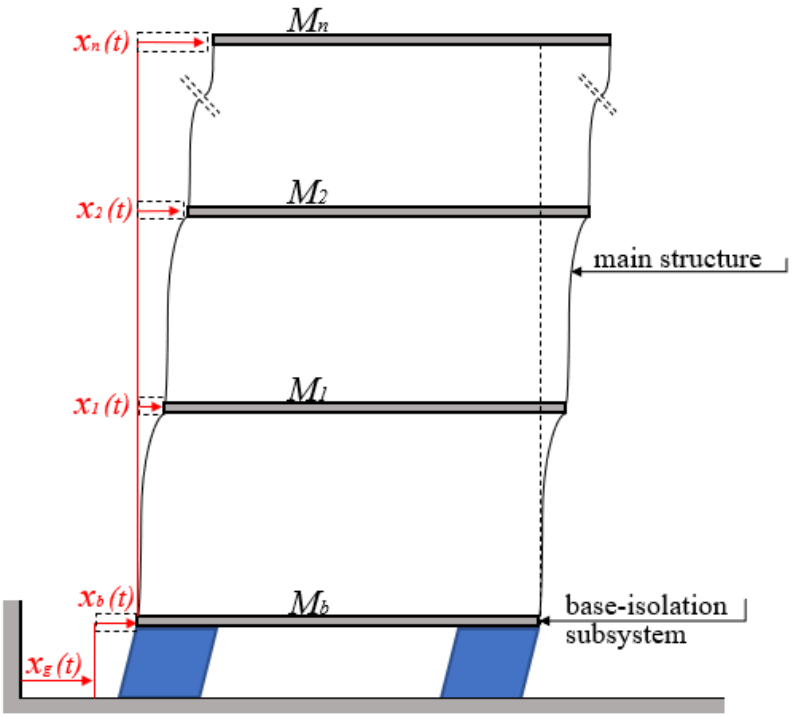

(b)

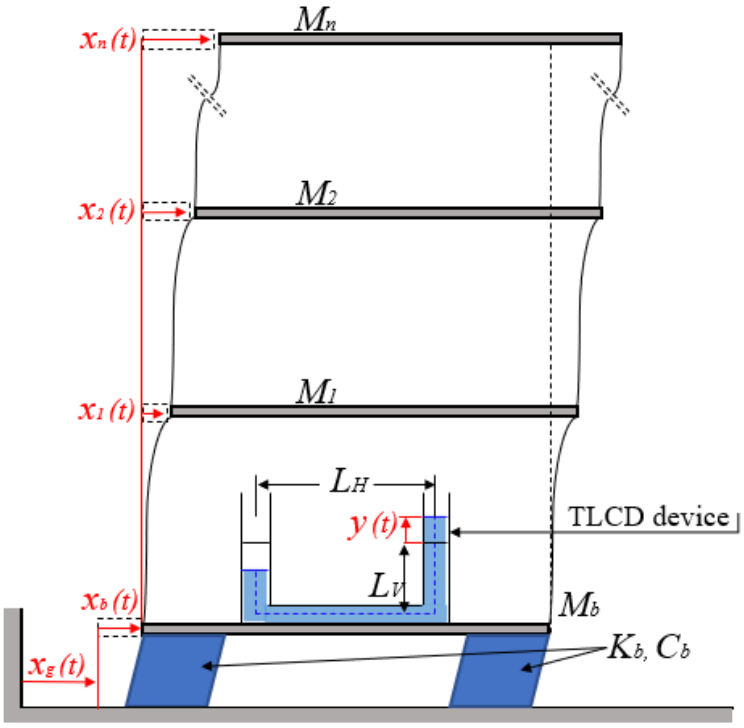

Figure 2 Base-isolated MDOF shear-type frame Structures: (a) without TLCD (b) with TLCD

Table 4: Properties Of Optimized TLCD System

Case no.			1	2	3
Maximum Limitation of Base Isolation's Displacement			40 cm		35 cm
Maximum Limitation of Base Isolation's Damping Ratio			40%	20%	20%
Controller Type	**Parameters**	**Units**	**Optimum Values**		
TLCD	*B*	m	10	10	6.297
	Beta	radian	1.31	0.84	0.89
	Cr	%	14.6	2.2	35.9
	H	m	10	10	7.88
	AH	m2	0.94	3.62	11.54
	AB	m2	0.01	2.96	17.76
	WTLCD	red/sec	0.14	0.67	0.88
	TTLCD	sec	44.7	9.32	7.18
	Mass Ratio (TLCD)	%	0.32	1.7	4.9
	Alpha	-	0.005	0.29	0.381
	Gamma	-	113.4	1.18	1.29
	K1	-	0.016	0.72	0.82
	K2	-	0.76	0.83	0.64

Among the FEMA P-695-FF record set, specifically two records involving earthquakes no. 21 and 37, are portrayed in figure (5), while comparison between the respective response time histories of the simple uncontrolled building and the base-isolated benchmark building with and without TLCD are shown in Figures 6 and Figure 7 for the roof and base levels under earthquake no. 37, and shown in Figure 8 and Figure 9 for the roof and base levels under earthquake no. 21, respectively.

Table 5: The Maximum Structural Responses of Base and Roof Levels Under 44 Earthquake Effects for The Hybrid Controlled Structure

Maximum Limitation of Base Isolation's Displacement			40 cm				35 cm	
Maximum Limitation of Base Isolation's Damping Ratio			40%		20%		20%	
Structural Response		**Units**	**Base**	**Roof**	**Base**	**Roof**	**Base**	**Roof**
Displacement	***Maximum***	cm	40	58.7	40	59.5	35	58.6
	Maximum Reduction by Using TLCD	mm	0.2	0.1	4.8	4.3	10	19
	Reduction Ratio	%	0.07	0.04	1.3	0.8	3.9	4.6
	Effectiveness Ratio	%	54.6	31.8	88.6	54.5	88.6	68.2
Acceleration	***Maximum***	m/s2	2.9	3.9	2.9	3.9	3.15	4.63
	Maximum Reduction by Using TLCD	m/s2	0.015	0.02	0.027	0.025	0.13	0.17
	Reduction Ratio	%	0.9	0.6	1.9	0.7	7.8	5.1
	Effectiveness Ratio	%	45.45	34.1	27.3	22.7	36.4	22.7
Interstory Drift	***Maximum***	mm	17	1.2	18	1.2	21.2	1.4
	Maximum Reduction by Using TLCD	mm	0.004	0.007	0.02	0.007	0.3	0.05
	Reduction Ratio	%	0.07	0.0007	0.14	0.7	2	5.2
	Effectiveness Ratio	%	13.6	34.1	11.4	20.4	18.2	22.7

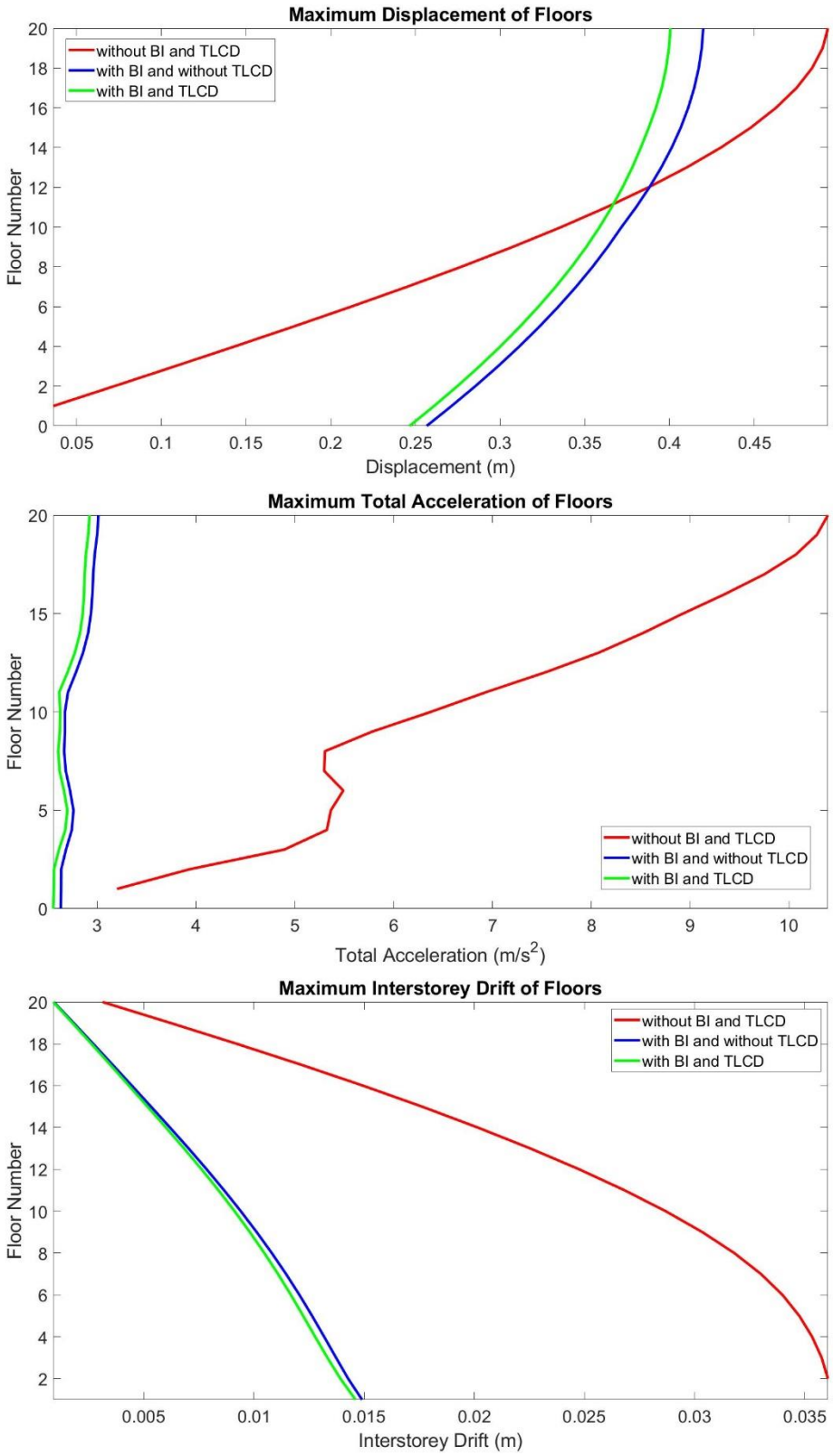

Figure 3 Peak Responses for hybrid-controlled structure, base-isolated structure and simple uncontrolled structure subjected to earthquake no.37 record

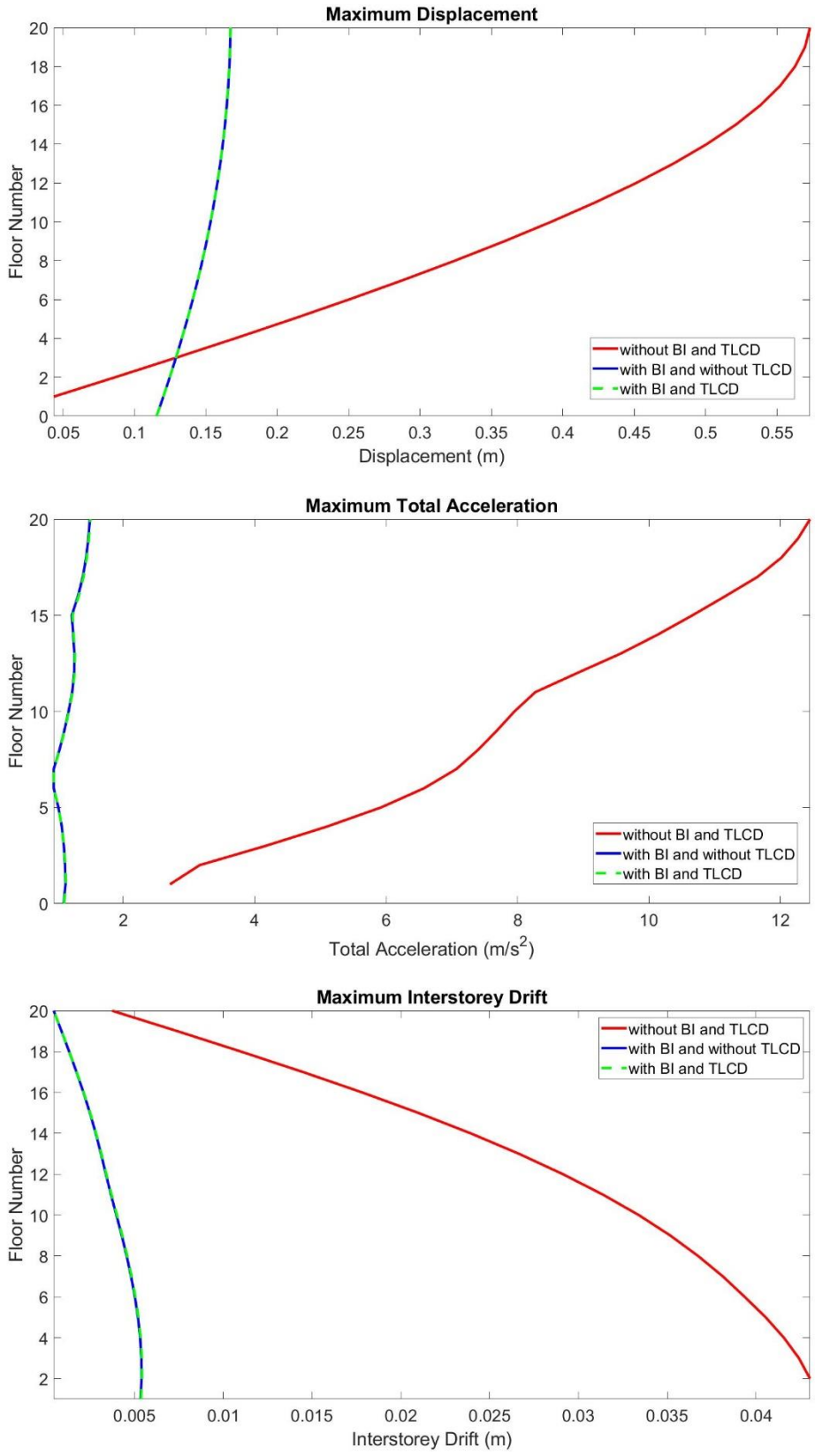

Figure 4 Peak responses for a hybrid-controlled structure, base-isolated structure and simple uncontrolled structure subjected to earthquake no.21 record

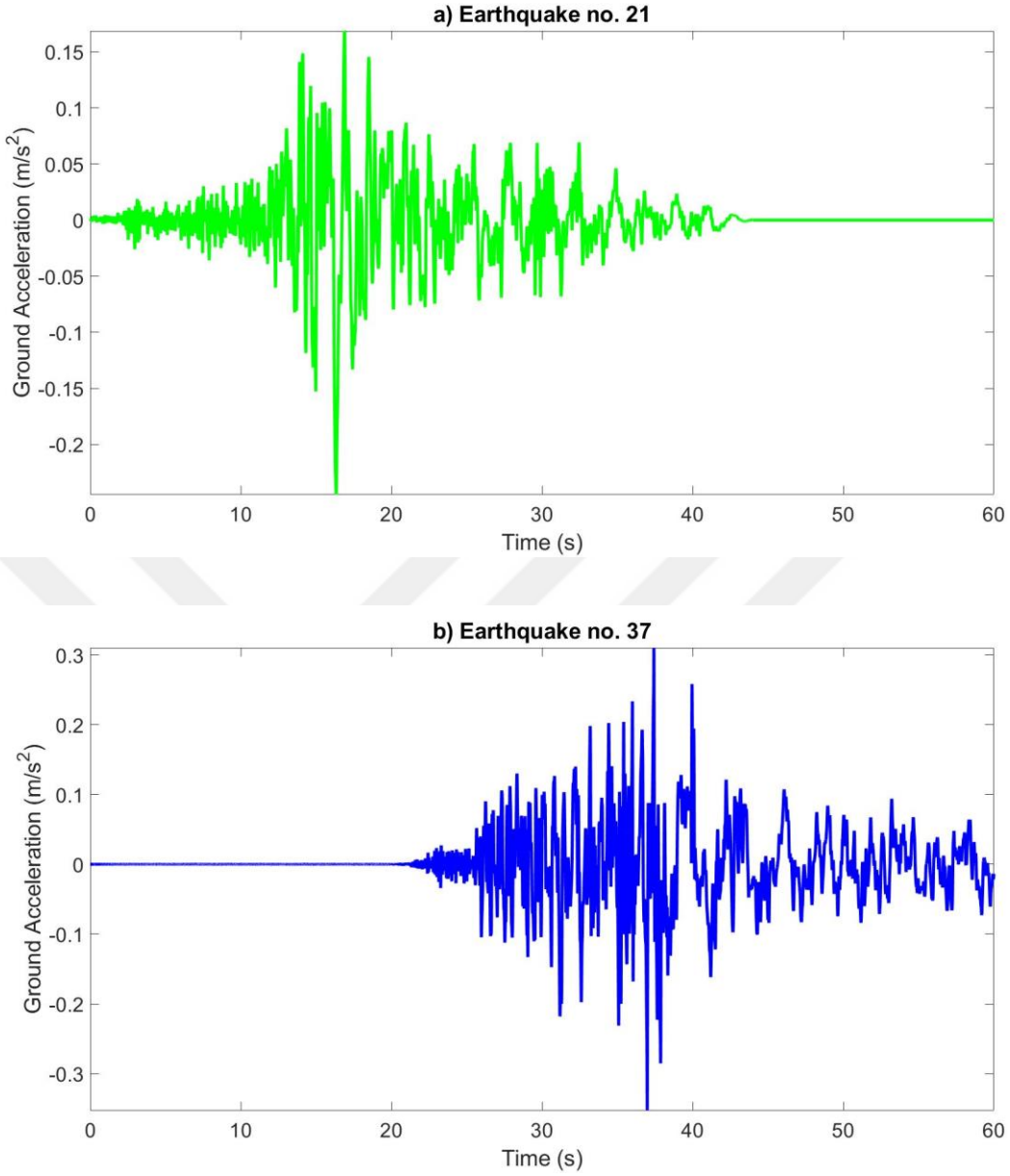

Figure 5 Two ground acceleration records of the FEMA P-695-FF set: a) Earthquake no.21; b) Earthquake no.37

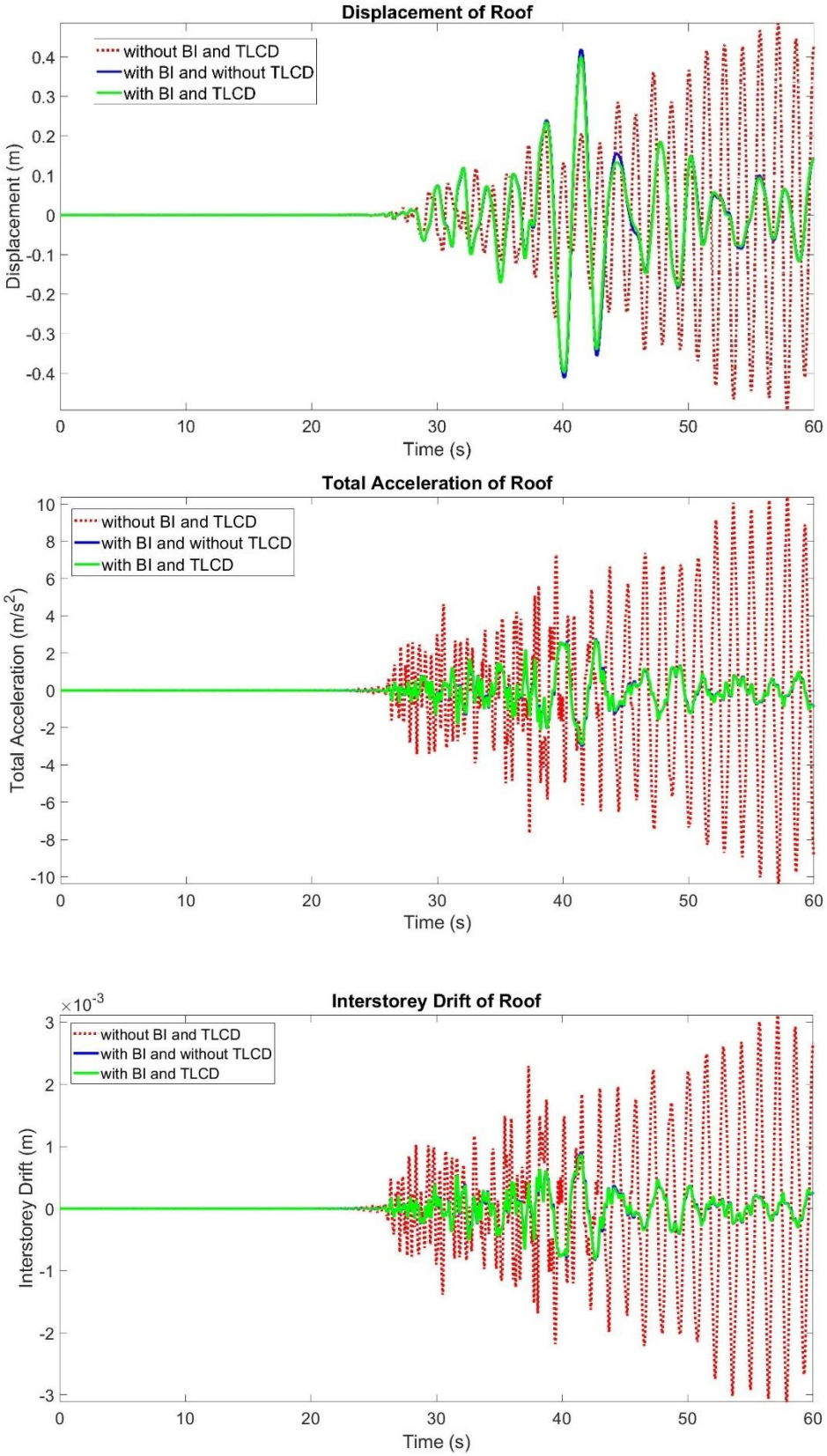

Figure 6 Response time histories of roof level for the earthquake-prone simple uncontrolled structure, base-isolated structure and hybrid controlled structure (earthquake no. 37 record)

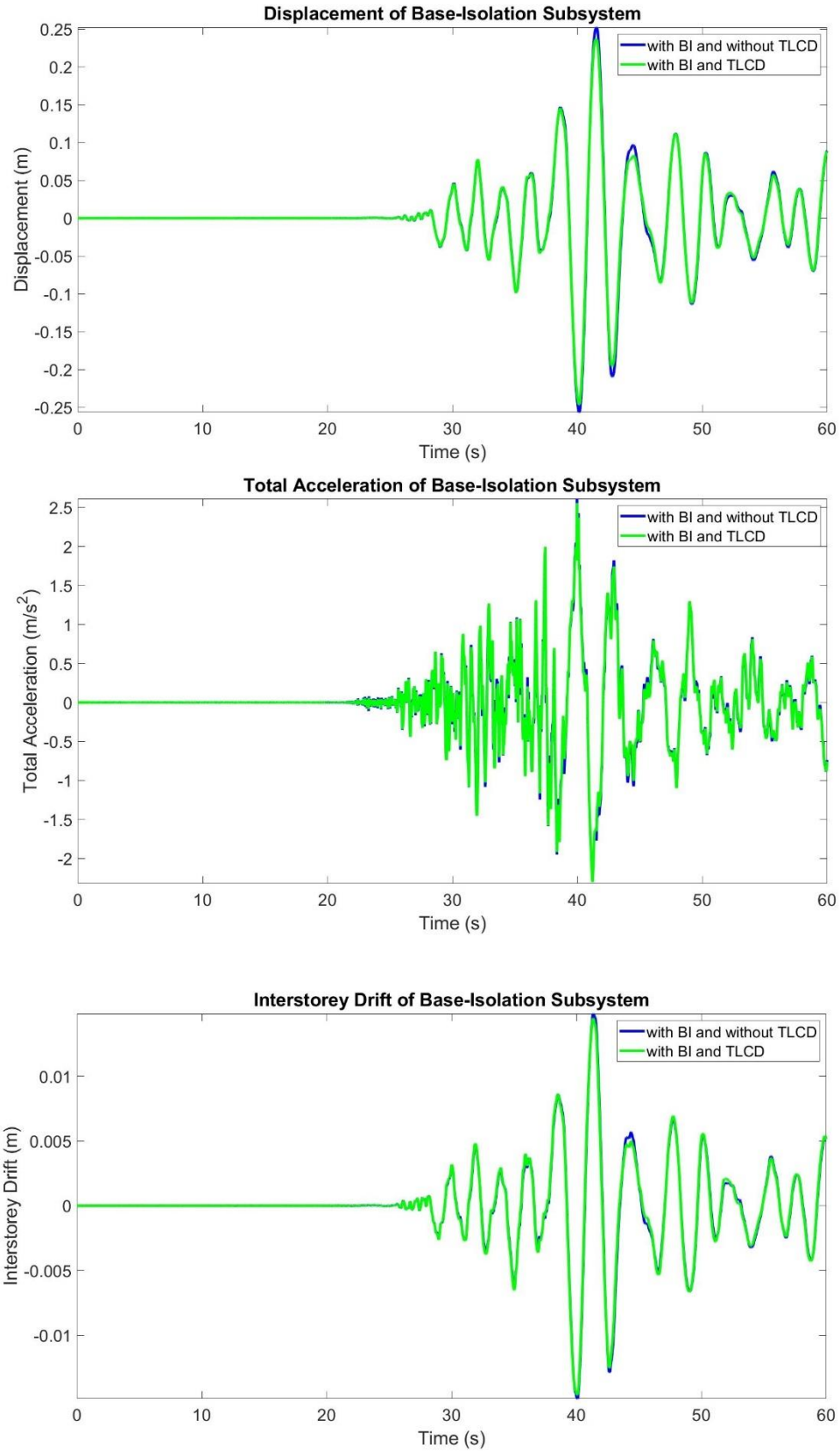

Figure 7 Response time histories of base level for the earthquake-prone simple uncontrolled structure, base-isolated structure, and hybrid controlled structure (earthquake no. 37 record)

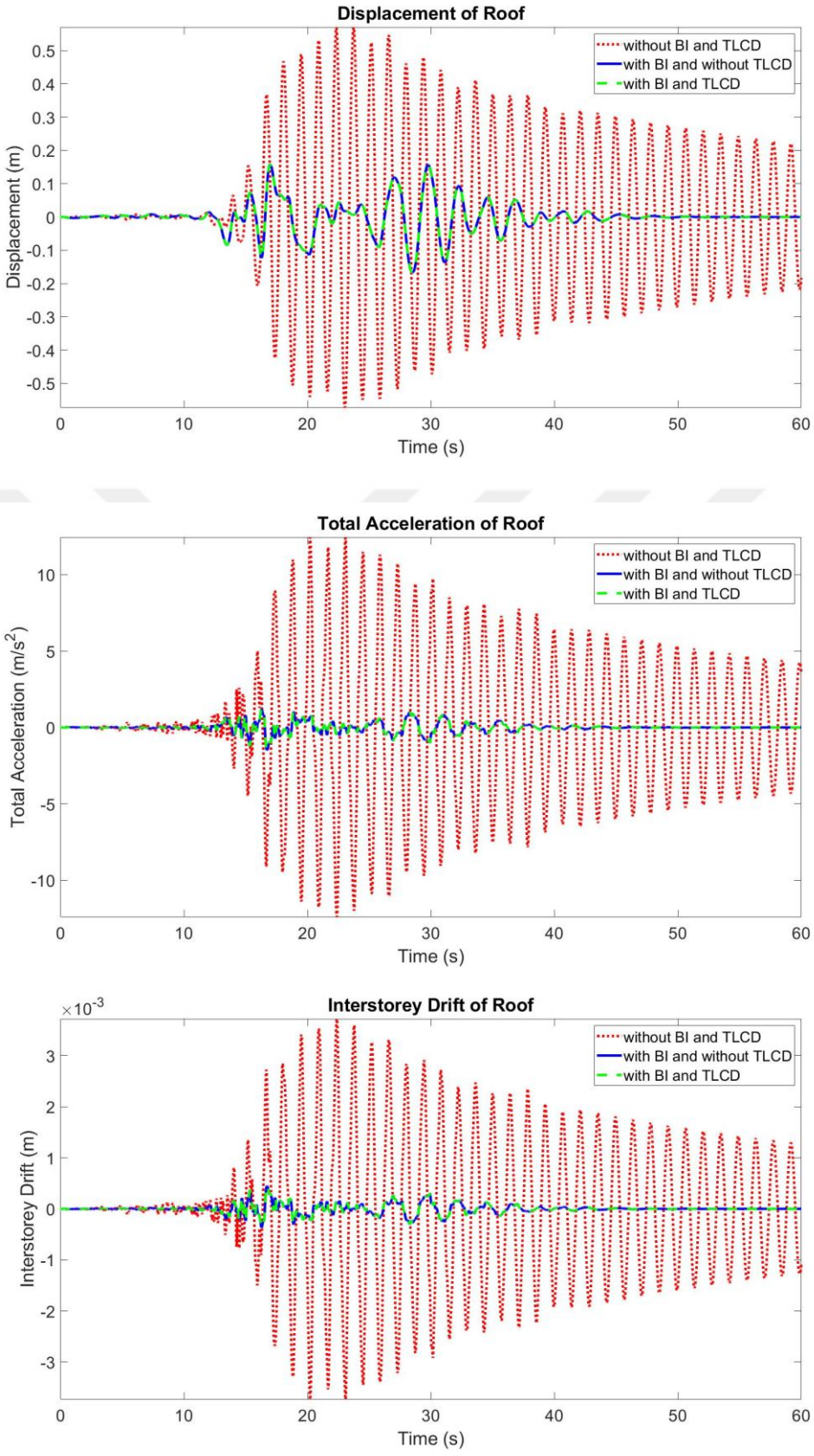

Figure 8 Response time histories of roof level for the earthquake-prone simple uncontrolled structure, base-isolated structure, and hybrid controlled structure (earthquake no. 21 record)

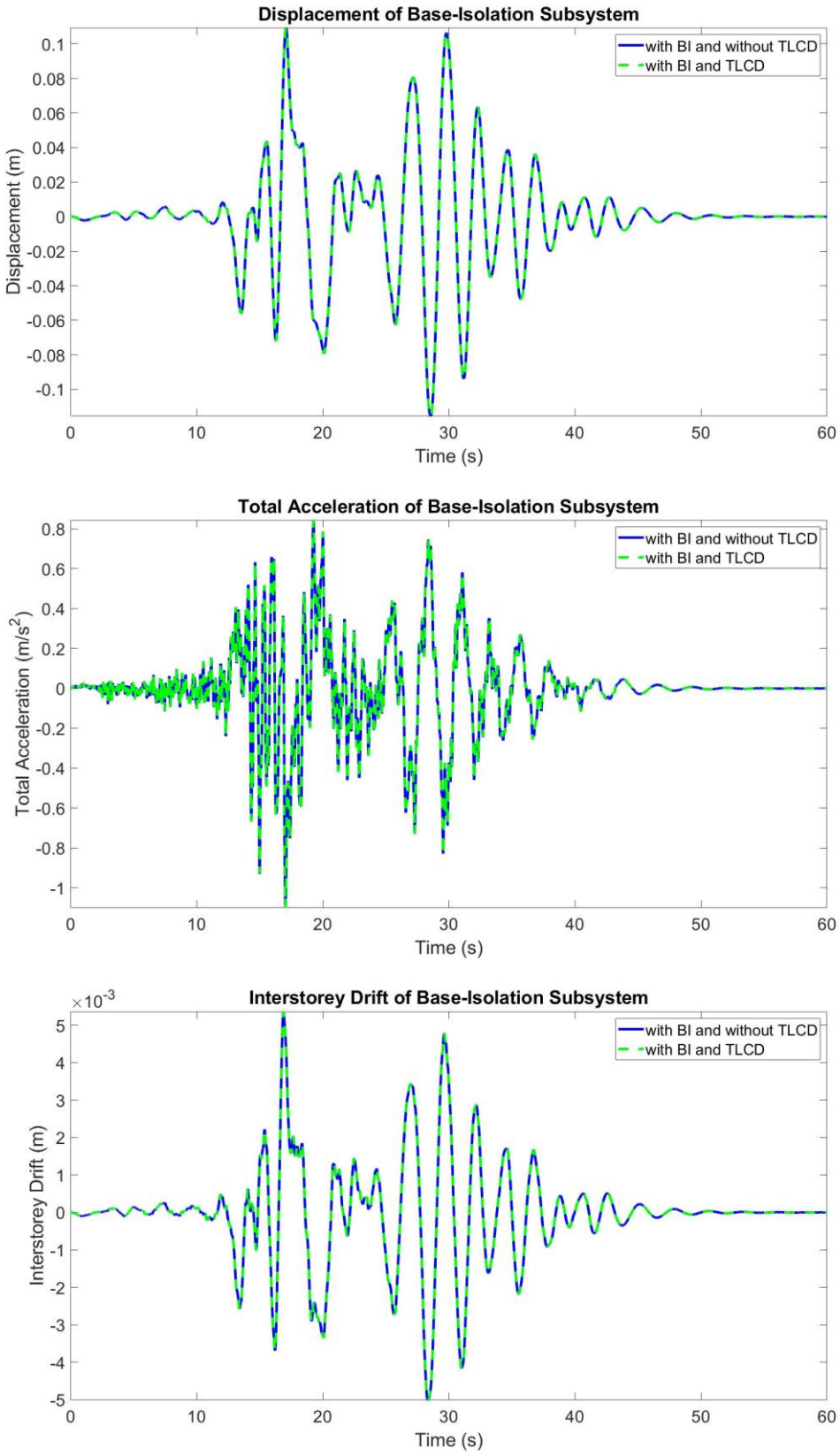

Figure 9 Response time histories of base level for the earthquake-prone simple uncontrolled structure, base-isolated structure, and hybrid controlled structure (earthquake no. 21 record)

5. DISCUSSION

It is observed that the fundamental natural frequency of the structure is reduced by the implementation of a base-isolation (BI) subsystem. As also observed from Table 2, the interstory drifts and total accelerations of the roof floor are clearly reduced for all cases. Although the displacements of the roof floor are reduced for most cases, using BI might cause a negative effect like in the case of earthquake number 38 where the displacement of the roof was increased. Based on the results in Table 2, It is believed that the benefit of deploying a base isolation subsystem to safeguard the structure has been amply proved. On the other hand, the responses of the base isolation subsystem are usually massive [20]. However, in our case, the BI subsystem's properties were optimized specifically for the investigated building which kept the displacements of BI below the maximum limitations. Nevertheless, displacements of BI might exceed the maximum limit in some cases such as in the case of earthquake number 38, where BI alone could not keep the maximum displacement less than 35 cm as shown in Table 2.

In addition, it is noticed from Table 2 that the interstory drifts and total accelerations of base and top levels have no noticeable change when connecting a passive TLCD to the base-isolation subsystem. However, in all the cases, displacements of the base and roof were reduced. But this reduction in some cases is very minor, not worthy to be mentioned, and in other cases the reduction value is noticeable but very small. For example, the reduction ratio of base displacements is between 0.02% and 3.9%. On the other hand, this small reduction has a very big effect in reducing BI subsystem displacements and keeping them below the maximum limit when the BI subsystem alone is not enough to control the structural response and keep it within the limits. Same as the case of earthquake number 38 where the displacement of the BI Subsystem without TLCD is 35.7 cm which exceeds the maximum limit of 35 cm. By using a TLCD system attached to the BI subsystem, the displacement was reduced to be equal to the maximum limit and thus the safety and integrity of the BI subsystem were protected.

The designs of the TLCD and base-isolation were specifically optimized, by using JAYA algorithm, for the 20-storey investigated structure. Moreover, both of the systems were

optimized considering using the other system in the structure. During the optimization process, two limitations were taken into consideration; The maximum displacement and maximum damping ratio of the base-isolation (Tables 3 and 4). The first case of optimization was with a maximum BI's displacement of 40 cm and a maximum BI damping ratio of 40%. The second case was with the same maximum displacement and 20% maximum damping ratio. The third case was for 35 cm maximum displacement and 20% maximum damping ratio.

As apparent in Figure 2, the optimized hybrid control system is able to effectively reduce the structural responses of the structure. The reduction at the roof reached to a maximum of 70.8% in displacement demand and 88% in acceleration and inter-story drift demands. The TLCD device when connected to the base-isolation subsystem could reduce the displacement demand of the base with a maximum reduction of 3.9%. It's important to emphasize that this slight decrease in base displacement can preserve the safety of the base-isolation subsystem. On the other hand, the inter-story drift and acceleration of the base were reduced in some cases and increased in other cases as shown in Table 2. However, the increment of inter-story drift and acceleration of base did not exceed 1.9% and the reduction could maximum reach 2.7%.

The time histories of all the response values can also reveal similar results. However, it is evident from a careful examination of the responses to each of the 44 records that there may be circumstances in which the TLCD has only a minor impact on lowering the base-isolation system's displacement.

Figure 7 for earthquake record number 37 shows that the peak base-isolation displacement has been significantly reduced by about 3.9% because of the TLCD device. Additionally, the peak roof displacement was decreased by nearly 18.9% (Figure 6). However, when taking into account the earthquake no. 21 record, a distinct tendency is apparent, as illustrated in Figures 8 and 9. In this instance, the TLCD device only reduces the peak base-isolation subsystem displacement by 0.02% (Figure 9). The buildings controlled by TMD [60] or the base-isolated buildings controlled by TMD [24,6] exhibit that behavior quite frequently. This is specifically because, in the initial few seconds after excitation, passive control devices (such TLCDs and TMDs) have a negligible effect on structural reactions. Thus, TLCD devices can not considerably lower the maximum displacement of the base-isolation subsystem if the

earthquake's strongest reaction comes early in the record, as it did in the instance of earthquake number 21. Utilizing an active TLCD would be advised for such excitation [7]. Despite this, the base-isolation subsystem's safety and integrity seem to be maintained while the displacement demand is reduced thanks to the passive control device.

As evident from Table 5, the maximum displacement of base did not exceed the maximum limitation in all cases. In addition, using TLCD system for the base-isolated structure was effective in reducing the displacement of base with minimum ratio of 54.6% and maximum ratio of 88.6% of the 44 earthquakes.

6. CONCLUSION AND RECOMMENDATIONS

The objective of this study is to develop a method to optimize the design of vibration control systems to ensure the safety of people, buildings and infrastructure during seismic excitations, and to prevent huge losses in the economic resources and capabilities of countries. In this context, control of high-rise building structures under seismic excitations was investigated using a passive hybrid control system consisting of a base-isolation subsystem and a passive TLCD system.

These control systems operate in order to dissipate the vibrations by lowering the responsiveness of structures like bridges to ground movements and winds. Aside from safety insurance, it also raises the standard of living for people who live or work in high-rise towers by not being exposed all the time to the feeling of the vibrations caused by wind actions. This study aims to find the optimum design for the passive hybrid control system to reduce displacements and protect the base isolators by implementing isolators and TLCD devices at the base level.

In this thesis, the metaheuristics methods will be used to establish the optimum design variables of base-isolators (stiffness and damping) and TLCD (shape properties to tune stiffness and damping). Metaheuristics have been successfully applied to TMD as a numerical optimization method including the members of this study [14-16]; however, an exact optimization using metaheuristics has not been proposed for the optimization of TLCD positioned in base-isolated structures. The challenge is in the need to consider the properties of both base-isolators and TLCD as design variables. The investigated metaheuristic was improved by modification according to the study's requirements. In addition, multi-cases of design constants were investigated to provide practical solutions to engineers.

Within the scope of this thesis, dynamic analysis of a benchmark model twenty-storey base-isolated TLCD-controlled structure was done by generating motion equations of the structure and the hybrid systems. These equations were then modelled utilizing Matlab with Simulink. Based on dynamic analysis of the structure and metaheuristic optimization methods, an optimization method was developed and a computer code was written. The optimization code

was generated for optimizing base isolation subsystem and the TLCD system considering using both of the systems in a structure under earthquake effects with tacking into account their properties as design variables. In this regard, one of the most suitable and successful metaheuristic algorithms which is known for its high performance was applied for designing both of the control systems. JAYA metaheuristic algorithm was used in the optimization process, particularly, similar to our example of base-isolated structures, to be ideal for systems with a low fundamental natural frequency dominant first mode.

The effectiveness of the optimized hybrid control system was investigated by performing numerical simulations and comparing the results with the simple base-isolated structure without TLCD. Finally, the performance of the base-isolated TLCD-controlled structure was evaluated by applying different recorded ground motions as base excitations. To evaluate the hybrid control system's performance, the performance of the base-isolated TLCD-controlled structure and to demonstrate the impact of the non-stationary nature of real ground motions, time-history analyses were performed on the FEMA P-695 far-field set's 44 recorded ground motions which are described in [35]. Furthermore, numerical simulations were performed on the controlled benchmark building by the hybrid control system, and the results were compared with the base-isolated structure without TLCD and the simple structure without control to investigate the effectiveness of the optimized hybrid control system.

Conclusions reached depending on the outcomes obtained from the study are summarized as follows:

1. The fundamental natural frequency of the structure is reduced by the implementation of a base-isolation subsystem.

2. The inter-story drifts and total accelerations of the roof floor are clearly reduced by using of base-isolation subsystem.

3. Although the displacements of the roof floor are reduced for most cases, using BI might cause a negative effect in which displacements of the roof have a chance to increase.

4. The responses of the base isolation subsystem are usually massive. However, in our case, the BI subsystem’s properties were optimized specifically for the investigated

building which kept the displacements of BI below or equal to the maximum limitations for most of the cases. Nevertheless, displacements of BI might exceed the maximum limit in some cases.

5. When a passive TLCD is coupled to the base isolation subsystem, there are no discernible changes to total accelerations and inter-story drifts of the base and top levels.

6. Base and roof displacements are lessened when a passive TLCD is coupled to the base-isolation subsystem. But this diminution in some cases is very minor, not worthy to be mentioned, and in other cases, the reduction value is noticeable but very small.

7. The small reduction in displacements of the base when connecting a passive TLCD to the base-isolation subsystem has a very big effect in keeping them below or equal to the maximum limit when the BI subsystem alone is not enough to control the structural response.

8. There may be instances where the TLCD has relatively little impact on lowering the base-isolation subsystem's displacement demand. This is specifically because in the initial few seconds after excitation, passive control systems (such TMDs and TLCDs) have a small impact on structural reactions.

9. The maximum displacement of the base did not exceed the maximum limit in all cases when coupled with a TLCD device.

10. Using TLCD system for the base-isolated structure was effective in reducing the displacement of the base with a minimum ratio of 54.6% and a maximum ratio of 88.6% of the 44 earthquakes.

According to the aforementioned findings, the TLCD device seems to be highly efficient in maintaining the safety and integrity of the base isolation subsystem. Besides, the proposed passive hybrid control system is able to effectively reduce the structural responses of the structure. The significant advantage of such a passive hybrid control system is that the passive TLCD system is easy to design, install and maintain, especially since the TLCD is on the ground level. We suggest as a future proposal for the researchers interested in completing the work done in this study to add another TLCD to be located on the roof level in addition to the proposed hybrid control system to overcome the possible negative effect.

REFERENCES

1. Fisco, N. R., & Adeli, H. (2011a). Smart structures: Part I—Active and semi-active control. Scientia Iranica, 18(3), 275–284. https://doi.org/10.1016/j.scient.2011.05.034

2. Fisco, N. R., & Adeli, H. (2011). Smart structures: Part II — Hybrid control systems and control strategies. Scientia Iranica, 18(3), 285–295. https://doi.org/10.1016/j.scient.2011.05.035

3. Buckle, I. G., & Mayes, R. L. (1990). Seismic Isolation: History, Application, and Performance—A World View. Earthquake Spectra, 6(2), 161–201. https://doi.org/10.1193/1.1585564

4. Kelly, J. M. (1999). The role of damping in seismic isolation. Earthquake Engineering & Structural Dynamics, 28(1), 3–20.

5. Barbat, A. H., Rodellar, J., Ryan, E. P., & Molinares, N. (1995). Active Control of Nonlinear Base-Isolated Buildings. Journal of Engineering Mechanics, 121(6), 676–684. https://doi.org/10.1061/(asce)0733-9399(1995)121:6(676)

6. Tsai, H.-C. (1995). The effect of tuned-mass dampers on the seismic response of base-isolated structures. International Journal of Solids and Structures, 32(8–9), 1195–1210. https://doi.org/10.1016/0020-7683(94)00150-u

7. Hochrainer, M. J., & Ziegler, F. (2006). Control of tall building vibrations by sealed tuned liquid column dampers. Structural Control and Health Monitoring, 13(6), 980–1002. https://doi.org/10.1002/stc.90

8. Ziegler, F. (2007). The Tuned Liquid Column Damper as a Cost-Effective Alternative for the Mechanical Damper in Civil Engineering Structures. The International Journal of Acoustics and Vibration, 12(1), 25–39. https://doi.org/10.20855/ijav.2007.12.1207

9. Di Matteo, A., Lo Iacono, F., Navarra, G., & Pirrotta, A. (2015). Innovative modeling of Tuned Liquid Column Damper motion. Communications in Nonlinear Science and Numerical Simulation, 23(1–3), 229–244. https://doi.org/10.1016/j.cnsns.2014.11.005

10. Di Matteo, A., Di Paola, M., & Pirrotta, A. (2016). Innovative modeling of tuned liquid column damper controlled structures. Smart Structures and Systems, 18(1), 117–138. https://doi.org/10.12989/sss.2016.18.1.117

11. Hochrainer, M. J. (2004). Tuned liquid column damper for structural control. Acta Mechanica, 175(1–4), 57–76. https://doi.org/10.1007/s00707-004-0193-z

12. Di Matteo, A., Lo Iacono, F., Navarra, G., & Pirrotta, A. (2014). Experimental validation of a direct pre-design formula for TLCD. Engineering Structures, 75, 528–538. https://doi.org/10.1016/j.engstruct.2014.05.045

13. Di Matteo, A., Lo Iacono, F., Navarra, G., & Pirrotta, A. (2012). The TLCD Passive Control: Numerical Investigations vs. Experimental Results. Volume 4: Dynamics, Control and Uncertainty, Parts A and B, 1283–1290. https://doi.org/10.1115/imece2012-86568

14. Bekdaş, G., & Nigdeli, S. M. (2011). Estimating optimum parameters of tuned mass dampers using harmony search. Engineering Structures, 33(9), 2716-2723. https://doi.org/10.1016/j.engstruct.2011.05.024

15. Bekdaş, G., & Nigdeli, S. M. (2017). Metaheuristic based optimization of tuned mass dampers under earthquake excitation by considering soil-structure interaction. Soil Dynamics and Earthquake Engineering, 92, 443-461. https://doi.org/10.1016/j.soildyn.2016.10.019

16. Nigdeli, S. M., & Bekdaş, G. (2017). Optimum tuned mass damper design in frequency domain for structures. KSCE journal of civil engineering, 21(3), 912-922. DOI 10.1007/s12205-016-0829-2

17. Geem, Z. W., Kim, J. H., & Loganathan, G. V. (2001). A new heuristic optimization algorithm: harmony search. simulation, 76(2), 60-68. https://doi.org/10.1177/003754970107600201

18. Rao, R. V., Savsani, V. J., & Vakharia, D. P. (2011). Teaching–learning-based optimization: a novel method for constrained mechanical design optimization problems. Computer-Aided Design, 43(3), 303-315. https://doi.org/10.1016/j.cad.2010.12.015

19. Kelly, J.M. (1986). Aseismic base isolation: review and bibliography. Soil Dynamics and Earthquake Engineering, 5(4), 202–216. https://doi.org/ 10.1016/0267-7261(86)90006-0

20. Yang, J. N., Danielians, A., & Liu, S. C. (1991). Aseismic Hybrid Control Systems for Building Structures. Journal of Engineering Mechanics, 117(4), 836–853. https://doi.org/10.1061/(asce)0733-9399(1991)117:4(836)

21. Palazzo, B., & Petti, L. (1997). Aspects of passive control of structural vibrations. Meccanica, 32(6), 529–544. https://doi.org/10.1023/a:1004244221103

22. Palazzo, B., Betti, L. (1999). Combined control strategies: base isolation and tuned mass damping. ISET J. Earthq. Technol. 36, 121–137.

23. Arfiadi, Y., S, H.M.N. (2000). Hybrid base isolation-passive mass damper systems. In: Computing in Civil and Building Engineering, pp. 279–286. Stanford, USA

24. Taniguchi, T., Der Kiureghian, A., & Melkumyan, M. (2008). Effect of tuned mass damper on displacement demand of base-isolated structures. Engineering Structures, 30(12), 3478–3488. https://doi.org/10.1016/j.engstruct.2008.05.027

25. Love, J., Tait, M., Toopchi-Nezhad, H. (2011). A hybrid structural control system using a tuned liquid damper to reduce the wind induced motion of a base isolated structure. Eng. Struct. 33(3), 738–746. https://doi.org/10.1016/j.engstruct.2010. 11.027

26. Adam, C., Hruska, A., Kofler, A. (2000). Elastic structures with tuned liquid column dampers. In: M. Durakbasa, A. Afjehi, P. Osanna (eds.) Proceedings of the of the XVI IMEKO (International Measurement Confederation) World Congress, vol. VII, pp. 351–356

27. Hochrainer, J.M. (2005). Tuned liquid column damper for structural control. Acta Mech. 175(1), 57–76. https://doi.org/10. 1007/s00707-004-0193-z

28. La Duc, V., Adam, C. (2016). General on-off damping controller for semi-active tuned liquid column damper. J. Vib. Control. https://doi.org/10.1177/1077546316648080

29. Ziegler, F. (2008). Special design of tuned liquid column-gas dampers for the control of spatial structural vibrations. Acta Mech. 201(1), 249–267. https://doi.org/10.1007/s00707-008-0062-2

30. Lin, S. M. (2016). "Nonlinear vibration control of a tall structure with tuned liquid column damper", Mechanics of Advanced Materials and Structures, Vol. 23, No. 2, pp. 146-15

31. M.C. Constantinou, T.T. Soong, G.F. Dargush. (1998). Passive energy dissipation systems for structural design and retrofit, Report MCEER-98-MN01, Multidisciplinary Center for Earthquake Engineering Research.

32. Ziegler, F. (1998). Mechanics of Solids and Fluids, (2nd Edition), Springer, New York, NY, USA

33. Liu, G., H., Li, H. N., and Guo, W. (2011). "An equivalent calculation method for analysis of structural vibration control of transforming TLD-structure to TMD-structure system." Engineering Mechanics, Vol. 28, No. 5, pp. 31-34.

34. Fu, C. (2018). Transforming Method of TLCD-structure to TMD-structure for Vibration Control. KSCE Journal of Civil Engineering, 22(4), 1384–1393. https://doi.org/10.1007/s12205-017-0287-5

35. FEMA P-695. (2009). Quantification of Building Seismic Performance Factors. Technical Representative, Federal Emergency Agency, Washington, D.C.

36. Di Matteo, A., Furtmüller, T., Adam, C. et al. (2018). Optimal design of tuned liquid column dampers for seismic response control of base-isolated structures. Acta Mech 229, 437–454. https://doi.org/10.1007/s00707-017-1980-7

37. Saifullah, M. K., & Alhan, C. (2017). Necessity and adequacy of near-source factors for seismically isolated buildings. Earthquakes and Structures, 12(1), 91–108. https://doi.org/10.12989/eas.2017.12.1.091

38. Chigira, M., Wu, X., Inokuchi, T., & Wang, G. (2010). Landslides induced by the 2008 Wenchuan earthquake, Sichuan, China. Geomorphology, 118(3–4), 225–238. https://doi.org/10.1016/j.geomorph.2010.01.003

39. Margesson, R., & Taft-Morales, M. (2010). Haiti Earthquake: Crisis and Response.

40. Chimamphant, S., & Kasai, K. (2015). Comparative response and performance of base-isolated and fixed-base structures. *Earthquake Engineering & Structural Dynamics*, *45*(1), 5–27. https://doi.org/10.1002/eqe.2612

41. Fu, C. and Ziegler, F. (2009). "Vibration prone multi-purpose buildings and towers effectively damped by tuned liquid column gas dampers." Asian J.Civil Engineering, Vol. 10, No. 1, pp. 21-56

42. Alhan, C., & Sürmeli, M. (2011). Shear building representations of seismically isolated buildings. *Bulletin of Earthquake Engineering*, *9*(5), 1643–1671. https://doi.org/10.1007/s10518-011-9293-z

43. Markou, A. A., Oliveto, G., & Athanasiou, A. (2016). Response simulation of hybrid base isolation systems under earthquake excitation. *Soil Dynamics and Earthquake Engineering*, *84*, 120–133. https://doi.org/10.1016/j.soildyn.2016.02.003

44. Garevski, M A (2012) ' Replacement of the Old Rubber Bearings of the First Base Isolated Building in the World', 15th World Conference on Earthquake Engineering (15WCEE)

45. Martelli, A., Clemente, P., de Stefano, A., Forni, M., & Salvatori, A. (2014). Recent Development and Application of Seismic Isolation and Energy Dissipation and Conditions for Their Correct Use. *Perspectives on European Earthquake Engineering and Seismology*, 449–488. https://doi.org/10.1007/978-3-319-07118-3_14

46. Nagarajaiah, S., & Erazo, K. (2016). Structural monitoring and identification of civil infrastructure in the United States. *Structural Monitoring and Maintenance*, *3*(1), 51–69. https://doi.org/10.12989/smm.2016.3.1.051

47. Erişgen, G. (2010). Depremin Geliş Açisinin Sismik Izolasyonlu Binalara Etkisi

48. Özdemir, S. (2016). INVESTIGATION OF SEISMIC ISOLATION EFFICIENCY FOR BUILDING STRUCTURES

49. Turkey Building Earthquake Code. (2018). Republic of Turkey Ministry of Interior Disaster and Emergency Management Authority, Ankara, Turkey

50. Hu, J. (2014). Response of Seismically Isolated Steel Frame Buildings with Sustainable Lead-Rubber Bearing (LRB) Isolator Devices Subjected to Near-Fault (NF) Ground Motions. *Sustainability*, *7*(1), 111–137. https://doi.org/10.3390/su7010111

51. Naeim, F., & Kelly, J. M. (1999). Design of Seismic Isolated Structures. *Design of Seismic Isolated Structures*. https://doi.org/10.1002/9780470172742

52. Nagarajaiah, S., Reinhorn, A. M., & Constantinou, M. C. (1991). Nonlinear Dynamic Analysis of 3-D-Base-Isolated Structures. *Journal of Structural Engineering*, *117*(7), 2035–2054. https://doi.org/10.1061/(asce)0733-9445(1991)117:7(2035)

53. Tena-Colunga, A., Eduardo Pérez-Rocha, L., Avilés, J., & Cordero-Macías, C. (2015). Seismic isolation of buildings for power stations considering soil-structure interaction effects. *Journal of Building Engineering*, *4*, 21–40. https://doi.org/10.1016/j.jobe.2015.08.001

54. Clemente, P., & Martelli, A. (2019). Seismically isolated buildings in Italy: State-of-the-art review and applications. *Soil Dynamics and Earthquake Engineering*, *119*, 471–487. https://doi.org/10.1016/j.soildyn.2017.12.029

55. Alhan, C., & Öncü-Davas, S. (2016). Performance limits of seismically isolated buildings under near-field earthquakes. *Engineering Structures*, *116*, 83–94. https://doi.org/10.1016/j.engstruct.2016.02.043

56. Alemdağ, E. C. (2016). A NEW METHOD TO INCREASE EFFECTIVENESS OF BASE ISOLATION ON TORSIONALLY UNRESTRAINED STRUCTURES. THE GRADUATE SCHOOL OF NATURAL AND APPLIED SCIENCES

57. Hitchcock, P. A., Kwok, K. C. S., Watkins, R. D., and Samali, B. (1997). “Characteristics of liquid column vibration absorbers (LCVA)-I.” Engineering Structures, Vol. 19, No. 2, pp. 126-134

58. Huo, L. S. and Li, H. N. (2012). “Structural vibration control using semi-active variable stiffness tuned liquid column damper.” Journal of Vibration and Shock, Vol. 31, No. 10, pp. 157-164

59. Reiterer, M., & Ziegler, F. (2006). Control of pedestrian-induced vibrations of long-span bridges. *Structural Control and Health Monitoring*, *13*(6), 1003–1027. https://doi.org/10.1002/stc.91

60. Tributsch, A., & Adam, C. (2012). Evaluation and analytical approximation of tuned mass damper performance in an earthquake environment. Smart Structures and Systems, 10(2), 155–179. https://doi.org/10.12989/sss.2012.10.2.155

FIRST PAGE OF THE PLAGIARISM REPORT

4801190879-Basel SALAAS

Yazar Elif ALTUNSU

Gönderim Tarihi: 13-Ara-2022 11:24PM (UTC+0300)
Gönderim Numarası: 1698682674
Dosya adı: YLTez.pdf (2.17M)
Kelime sayısı: 13592
Karakter sayısı: 77065

ETHICS COMMITTEE PERMISSION

WARNING: It is mandatory to obtain an Ethics Committee Permission for all research topics related to living subjects.

☐ **Ethics Committe permission is required.**

☒ **Ethics Committe permission is not required.**

Basel SALAAS

(Signature)

INSTITUTIONAL PERMISSIONS

WARNING: It is mandatory to obtain Institutional Permission for all research topics related to living and dead subjects. In cases involving confidentiality and privacy, the name of the institution should be closed.

☐ **Institutional permission is required.**

☒ **Institutional permission is not required.**

Basel SALAAS

(Signature)